Mehhatroonikainstituut

mehhatroonika osakonna juhataja

MHK70LT

Uljan Sinani

Must räni päikesepatarei rakendustes

Magistrikraadi lõputöö

Autor taotleb

tehnikateaduste magistri

akadeemilist kraadi

Tallinn

2016

Department of Mechatronics

Chair of Mechatronics department

MHK70LT

Uljan Sinani

Black Silicon for Solar Cell Applications

MSc thesis

The author applies for

The academic degree

Master of Science in Mechatronics engineering

Tallinn

2016

AUTHOR'S DECLARATION

I declare that I have written this graduation thesis independently.

These materials have not been submitted for any academic degree.

All the works of other authors used in this thesis have been referenced.

The thesis was completed under Professor Mart Tamre supervision

"MHE" 2016

Author: Uljan Sinani

Signature:

The thesis complies with the requirements for graduation theses.

"MHE"....................2016

Supervisor: Professor Mart Tamre

Signature: ……………………

Accepted for defense.

Chairman of the defense committee.................................

"..."....................201….

Signature.............................

MASTER'S THESIS SHEET OF TASK'S

Year 2016 semester, (Spring)

Student: Uljan Sinani, a144753
Curricula: MAHM02/13
Specialty: Mechatronics
Supervisor: Professor, Chair of department, Mart Tamre
MASTER'S THESIS TOPIC:
Supervisor: Professor, Chair of Mechatronics department, **Mart Tamre.**

Advisers: **Jakob Kjelstrup-Hansen**, Associate Professor NanoSYD, +4565501685.

Luciana Tavarez, Assistant Professor NanoSYD, +4565501645.

(In English) Black Silicon for solar cell applications.

(In Estonian) Must räni päikesepatarei rakendustes.

Assignment to be completed and the schedule for their completion:

Nr	Description of tasks	Timetable
1.	Operatio and control parameter for ICP RIE Machine (plasma etching).	Week 5 – 6
2.	Silicon etching, characterization of microstructures (textures).	Week 7
3.	Study of geometrical and size of the textures (trenches).	Week 8 – 9 – 10
4.	Light reflection measurement and efficiency in light absorption for black silicon.	Week 11 – 12
5.	Final compilation and future work.	Week 13

Solved engineering and economic problems: Through this thesis work, I aim to measure light reflection in black silicon, and inspect different Nano textures created through plasma etching using silicon. Thereby analyzing the light absorption efficiency as a means to apply the anti-reflection layer in solar cell applications. So through this study the aim is to better understand the properties and fabrication process of black silicon as a way to have better efficient solar cells, that can be used for big solar cell companies and customers, of different categories at a low cost.

Language: English

Application is filed not later than **12/02/2016**

Deadline for submitting the thesis 01/06/2016

Student Uljan Sinani   /Signature   /date: 11**/02/2016**

Supervisor Mart Tamre   /Signature   /date: **Feb 10th, 2016.**

Table of Contents

EESSÕNA

Antud magistritöö teemal „Silikoon päikseelementide rakendustel "on esitatud täitmaks Tallinna Tehnikaülikooli magistrikraadi saamise nõudeid. Projektitöö oli teostatud kasutades SDU NanoSyd-i Mikro- ja Nanotehnoloogia osakonna seadmestikke ning töökeskkonda minu akadeemiliste õpingute ajal, mis kestsid vahemikus september 2015 kuni mai 2016.

Ma soovin tänada Tallinna Tehnikaülikooli võimaluse eest töötada antud diplomitöö kallal ende täieliku toe ja heakskiiduga. Samuti soovin tänada minu peajuhendajat professor Mart Tamret, kes andis mulle tuge, juhendust ning julgust töötada diplomitöö kallal olles vahetusõpilane. Tänan ka teisi juhendajaid, Jakob Kljestrup Hansen ja Luciana Tavares SDU NanoSyd-ist, kes olid väga abivalmid kogu tööprotsessi ajal. Tahan tänada koristusmeeskonda, kes hoidsid töökeskkonda SDU NanoSyd-is puhtana ning kasutusevalmina, ning ma olen samuti tänulik nende valmiduse eest aidata seadmete kasutamisega ja probleemidega.

Samuti soovin ma tänada oma kohapealset koordinaatorit Arkadiusz Jaroslaw Goszczak abi ning ka kiire vastamisaja eest siis, kui mul tekkisid probleemid seadmete kasutamisega. Viimasena järjekorras, kuid mitte tähtsuse poolest, ma soovin tänada oma perekonda kogu toe ning julgustuse eest, mida nad mulle andsid. Ja ka NanoSyd-i meeldiva ning puhta töökeskkonna eest.

1 INTRODUCTION

High demand for renewable energy sources as a form of clean energy and, in particular, solar energy has led to new developments made on silicon solar cell applications for energy harvesting. Nowadays silicon solar cells make about 80% of the commercial solar cells. Which means that Silicon is the main element used in solar cell production. Silicon, as the second abundant element [1] on Earth, cheap and being mature in fabrication techniques it is used in semiconductor technology for microelectronics and nanotechnology applications. Thus, for using it we are aiming at good efficiency, flexibility, and low cost, important for so many applications in semiconductor technology and other areas. Particularly in our case, we try to exploit Silicon properties as an element for producing Nano-structures used in solar cells to increase the efficiency by special etching techniques [2].

The Nanostructures in solar cells are used as a means of increasing the light absorption and internal reflection. Later on this material, we will describe and focus on the methods used and developed to improve the light absorption, through some Nanostructures that are known as grating. The Gratings are utilized to form the anti-reflection coating in solar cells and are critical for producing efficient solar energy modules. So the applications used for solar cells, rely on Silicon processing and as a technique with low cost, black silicon method has proven to bring the solar cells commercially available with a low cost. Moreover, the application of the black silicon is not only and limited to solar cells but it has found a wide range of applications in other fields too, related with:

- Solar cells and light-emitting devices.

- Micro-electro-mechanical systems (MEMS).

- Chemical and bio-sensors.

- Optoelectronic and photonic devices.

Sissejuhatus

Suur nõudlus erinevate taastuvate energiaallikate vormide, puhta energia ja eelkõige päikeseenergia järele on viinud uute arenguteni must räni päikesepaneelide rakendamisel. Tänapäeval moodustuvad must räni päikesepatareid umbes 80% kaubanduslikest päikesepatareidest, mis tähendab, et must räni on peamine element päikesepatareide tootmisel. Must räni, kui teine levinum element Maal, odav ja tootmistehnikas kergesti töödeldav, on kasutusel pooljuhttehnoloogia alal mikroelektroonika ja nanotehnoloogia rakendamisel.

Kasutades must räni püüame saavutada head efektiivsust, paindlikkust ja odavust, mis on oluline paljudes pooljuhtide tehnoloogiarakendustes ning teistes sarnastes valdkondades. Eriti meie puhul, püüame kasutada must räni häid omadusi kui nanostruktuuride tootmisel päikesepatareides spetsiaalse söövitusmeetodite abil [2].

Nanostruktuuride kasutamine päikesepatareides suurendab valguse neeldumist ja sisepeegeldust. Lisaks kirjeldame ja keskendume meetoditele, mis on kasutusel ja arendamisel, mis aitavad parandada valguse neeldumist läbi mitmete nanostruktuuride, mis on tuntud kui (grating) mõiste all. The grating (võre) kasutatakse peegeldumisvastase katte moodustumise eesmärgil päikesepatareide pinnal ning on tähtsad tõhusama päikeseenergia moodulite tootmisel. Erinevad meetodid päikesepaneelide rakendamisel tuginevad must räni headele omadustele ja odavusele, mis teeb võimalikuks musta must räni saadavuse madala hinna eest. Lisaks sellele on ränile leitud kasutust mitmetes teistel valdkondades.

-päikesepatareid ja valgust kiirgavad seadmed

-Elektromehaaniline mikrosüsteem

-keemia- ja biosensorid

-optilis ja fotoonikaseadmed

Abbreviations and Acronyms

ICP- Inductively coupled Plasma

RIE – Reactive Ion Etching

ICP RIE – Inductively Coupled Plasma Reactive Ion Etching

CVD – Chemical Vapor Deposition

PECVD – Physical Etching Chemical Vapor Deposition

RF – Radio Frequency

SEM – Scanning Electron Microscopy

AFM – Atomic Force Microscopy

bSi – Black Silicon

a-Si – Amorphous Silicon

AR – Antireflection Coating

ARC – Anti-reflection Coating

HF – Hydrofluoric acid

SF$_6$ – Sulphur fluoride

ALD – Atomic layer deposition

PV – Photo Voltaic

WCA – Water Contact Angle

2 MOTIVATION

The challenges faced nowadays concern the usage of fossil fuels and reduction of prices for the oil or natural gas. Thus, going for renewable energy sources is a desired alternative to reduce emissions. hence, finding the right combination of sources and utilizing them in the right way could be one path to go. This motivates me to contribute to solving energy sustainability problems. That drives the research for renewable sources like solar power. Which is clean, abundant and important for life on earth.

Among alternatives to harvesting the solar energy, coming in different forms, be it photonic or thermal energy. My focus and interest are in the conversion of its photon energy into electrical energy. And Solar cells have proven to be the desired candidates for this process. Converting the sunlight energy that is hitting the Earth's surface into electricity, creates the possibility of harvesting a part of it from an energy density of 1,000 W/m2. For this purpose, both inorganic and organic solar cells are being researched to finding ways to make them more efficient and cost-effective. Where combined both a higher efficiency and a lower cost are a more difficult challenge. To achieve it the right mindset, tools and technology could lead to the solution. Inspired by this concept I started to work on this project approaching to one side of this challenge. Hence started to study the properties of black silicon for solar panels.

The method chosen to tackle the challenges and problems related to black Silicon was to consider an effective method that would control the properties of black Silicon and find a method to reduce the time for fabricating it. From this point the plasma etching method was chosen, for creating the Nanostructures in less time than conventional grating while granting controllability in the etching process. As means to study the etching process and know-how to control the geometry for the nanostructure, by controlling the absorption and reflectivity from the black silicon layer, applied on top of solar cells.

2.1 This project

The purpose of this project is to fabricate the Nanostructures, important for light absorption on the upper layer of solar cells. They are created through the black silicon method, to form the layer with the same name called 'black Silicon'. Thus with the aim to improve the absorption of the photon energy from the sun and minimize reflectance. Specific shape, size and density of these Nanostructures is to be tested. For their development the ICP RIE plasma etching machine was used. Where depending on various variables such as gas, chuck bias, RF power etc. various features of Nanostructures can be controlled. So, aiming at a lower reflection rate from the black silicon surface, I reviewed the previous research work related to black silicon and state of the art texturing techniques.

The work started with some simple recipes, and then through a specific framework, I tried to reach the best combination to fabricate the black silicon. Also understanding the physics behind the black silicon development to increase the chances for better light absorption rate. Albeit efficiency was not the only target in the fabrication of black Silicon. Finding a cheaper way to fabricate it was also part of the work. This came eventually since the conventional texturing methods on solar cells, involve much more time and cost to make the anti-reflection coating.

Through this project, the right support and tools were given to conduct my experiments that were in conjunction with another course of nanotechnology profile, called Nano-project. So basically, I had the challenge and I had to find my way working to further contribute in an area important for future renewable energy sources like solar energy.

2.1.1 Thesis organization

The thesis is organized in three main parts, starting with the theory about the surface science techniques for texturing, and its fabrication methods. Literature review about etching methods and tools. The last part, consists in an introduction to black silicon method and tools used to fabricated it, ending with the actual results from this project work. For each section results and discussions will take place. The work is divided such that the theory forms the ground for the practical work. Creating a better understanding of the applied methods. Then, illustrations for each step and tool used are shown in conjunction with the working principle of the device(s) or process described. The next layer is the presentation of the data gathered during the work. Shown in combination with graphs, tables and figures to representing the full work done in this project.

All the data process, follows the workflow I used for the completion of this thesis work. So to briefly introduce the next chapter. Some background is introduced about the work of ICP RIE machines, how they work and how to control them for a specific process. Next the characterization of the black silicon Nanostructures will be done in SEM. Then, equipment and tools will take place to recap the methods and tools used, for measuring the black silicon properties. In the same section, the work done for the project will be explained in detail. Starting from the analysis in SEM to reflectivity test till the 'Bosch process' and Water Contact Angle (WCA). In the last part the final results of this work will be presented and an overview of the accomplishments achieved.

2.2 State of the art techniques.

The field of Nanotechnology recently has evolved exponentially into achieving higher resolution in nanoscale. Lithography methods are being developed to transfer even smaller feature size elements into substrates [1]. Thus Extreme Ultraviolet Lithography (EUV) [2], Electron Beam Lithography (EBL) [3], Nano imprint lithography [4] but also thin films can be deposited accurately in the scale of several nanometers for fabricating microelectronic devices. As an example, a typical layer of 1nm and the linewidths of 100 nm are good achievements, striving to exploiting and going further deep on Nano dimensions [5].

As lithography has evolved so do depositing and etching techniques to create and control different layers have evolved. Hence for high precision patterning composed of several layers, the deposition and etching should be very accurate [6]. For this work the focus is to use an effective etching method, using state of the art techniques for both dry and wet etching process. To achieve good etching using the latest available tools plasma machine was the alternative. The type of plasma machine that was used for etching is Inductively Coupled Plasma Reactive Ion Etching (ICP RIE) [7]. This technique for the etching process, relies on the reactive species formed by the association of gasses in a plasma, and the adsorption on the substrate surface. It reacts with the substrate atoms to form volatile compounds that later desorb and move away when the etching stage finishes. Note that the plasma on this machines is generated by a radio frequency (RF) electric field [8].

So the dry etching technique is a good method that can lead into creating high precision structures. Some recent challenges related to dry etching are the ability to control the etching direction, etching rate and selectivity[1]. Though to control the etching variables a combination of methods is necessary. Bosch process has been a breakthrough in the etching techniques used in lithography for patterning or MEMS[2] devices. It is used to etch deep in the substrate while maintaining the directionality in etching [9].

---

[1] The ability to etch a specific layer, say Silicon and inability to etch SiO_2
[2] Micro-Electro-Mechanical Systems

While lithography and etching push the limits to going further into atomic scale, some limitations are increasing as well. The feature size of elements becomes critical as we go down in scale, that is due to atomic forces interacting in the structure [10]. Thus Moor's law starts to break at the limit of atomic scale, since the physic rules as we progress deeper in nanoscale will be different. This is when dealing with quantum mechanics, which will be inevitable for the future of nanotechnology as a field, and methods to operate in its scale [11].

2.2.1 Surface science

Surface science is the study of the chemical and physical interfaces for liquid state, physic or combined. Hence including all the combination from solid to gas till solid to vacuum interfaces. The importance of surface science relies on its ability to explain the processes created on different states of the materials. Also able to understand the properties of the substances in the interface or explaining the physics behind different scanning microscopy techniques such as scanning tunneling microscopy [12].

Thus surface science is important with the right tools into working at the nanoscale. Allowing us to not only to observe the small scale but also manipulating it. Hence applying thin films, nanoparticles, nanowires, quantum dots etc. to improve the bulk properties of the materials. Allowing to better control the physical properties of the materials in different levels. An example would be the interaction of these layers carrying the charges in the interface between different materials, the case of solar cells [13].

To conclude such interfaces like liquid surface tension, water contact angle, silicon surface interaction, adhesion etc. [14] are important when entering the micro and nanoscale. Thus allowing to predict the physical and chemical behavior of the processes at the interface, like etching, crystal growth, epitaxial processes etc.

2.2.2 Surface texturing techniques

Surface texturing is the methods of transforming the physics of a surface. Mainly related to surface roughness, characteristics of lay, waviness etc. It determines the interface physics and controls the surface profile. For profile control like in lithography, a combination of dry and wet etching methods is required. Particularly, for surface texturing used in photovoltaics the lithography method is commonly used for surface texturing.

 It is preferable to use specific etching techniques when a certain surface texture is required. The techniques used start from lithography patterning, wet etching, dry etching etc. Basically we apply texturing by removing material from the bulk in a specific pattern or surface profile. Thus, creating textures takes time and good control of the structures in micro-scale. While limiting the mass production efficiency in some cases i.e. when we use the photolithography technique many times [15].

As an effective way for texturing multi-crystalline wafers, ion etching is used. Although more in detail will be treated later when talking about the uses of the reactive ion etching (RIE). In principle it can create surfaces with high absorption or low reflectance, even in various orientations of the grains in crystalline. Hence a good texturing contributes to a higher efficiency of large area multi-crystalline silicon solar cells [16].

In this work the aim is to remove this texturing step that is conventionally used in the fabrication of solar cells and replace it with the black silicon method. As an effective way to produce regular Nanostructures with specific shape, size and density. Utilizing the plasma ion etching techniques that combine dry and wet etching [17].

3   LITERATURE REVIEW

Referring to the work and research done by the techniques applied on surface treatments. It is evident that the time it takes to create the textures be they for coating, depositing or etching [18]. Most of these processes require time and are costly to apply, especially when etching, which this thesis work is concerned [19]. So the method for creating these efficient textures (Nanostructures) useful for light absorption and scattering in our context are not easy to achieve. The way how these texturing techniques start is different. But what is being researched and applied are the grating methods done with lithography and ion etching [20]. The results achieved are different for any technique applied to create the gratings. So, the purpose of reviewing in the literature for anti-reflection coating methods, is to understand and find the best anti-reflection coating, where the black silicon method was considered effective for a lower reflection rate [21]. For the etching methods plasma etching, was known to be a quick and efficient process to create anti-reflection coatings [17].

Hence, the results in the end, will tell which is the best methods to create the Nanostructures, therefore black silicon in this case. When dealing with wet etching solvents or wet chemicals substances to a specific pattern a good controllability of the process is required. The chemicals that one has to deal with in the wet etching, usually consist of hydrofluoric acid (HF) or potassium hydroxide (KOH). Both are dangerous but the most is HF, thus has to be used very carefully in the process when etching [22]. So these chemicals should be used in a controlled environment and with proper safety precautions in consideration. When considering the dry etching the procedure is based from the ratio of gases such SF_6, O_2, Cl_4, Ar etc. The plasma is created due to the electromagnetic field which is able to accelerate ions, core of the dry etching process [23]. To conclude it is said that both methods wet and dry etching have pros and cons, though dry etching is more safe and controllable but having a higher cost of process [24].

3.1 Theory of Plasma etching

So plasma etching allows us to etch anisotropically and create much sharper structures and control the etching rate via ions driven from the RF field. The etching process via plasma is shown in the figure 3.4.
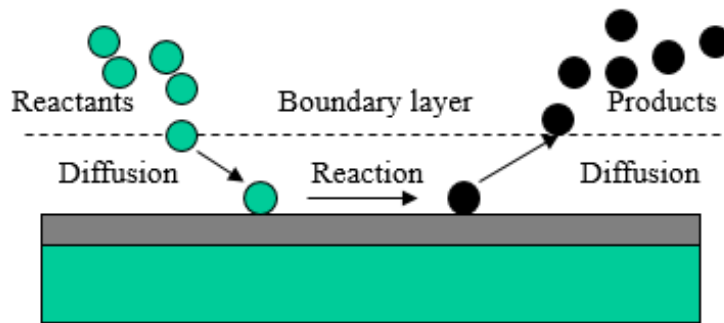

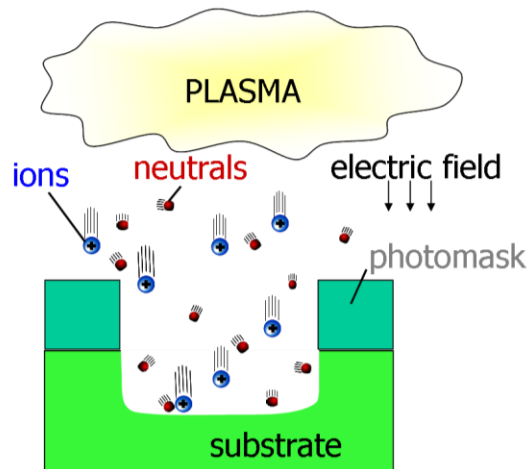Figure 3.1 Fabrication Engineering at the Micro- and Nanoscale [14]

Figure 3.2 Ion and neutral species from a plasma, reaching the substrate [16]

For a better understanding of the etching process on the substrate and the way, specimens hit the sample refer to figure 3.5. Where an electric field accelerating the specimens and the ions while they hit the sample can be seen.

The etching process is a consequence of ions hitting the surface of the wafer, and due to their high mass and therefore inertia, a vulnerable reaction takes place. With the consequence of creating anisotropic walls and etching deep on the substrate. Whereas, in the case of the wet etching, the reaction to etch away the material, occurs same time as the liquid touches the surface of the sample [11].

Considering the main advantages of plasma etching over the wet etching one can see that there are two main reasons why plasma or dry etching is more commonly used. One reason is that very reactive chemical species are produced in a plasma that etches more vigorously than species in a non-plasma environment. Another reason is related to the fact that directional or anisotropic etching is possible with a plasma to etch. Where directional etching is needed to minimize under etching and etch bias. Plasma etching systems can be designed so that either the reactive chemical components or the ionic components dominate here in most cases the combination gives a better result. The plasma machine interface used for this work is shown in the figure 3.6.
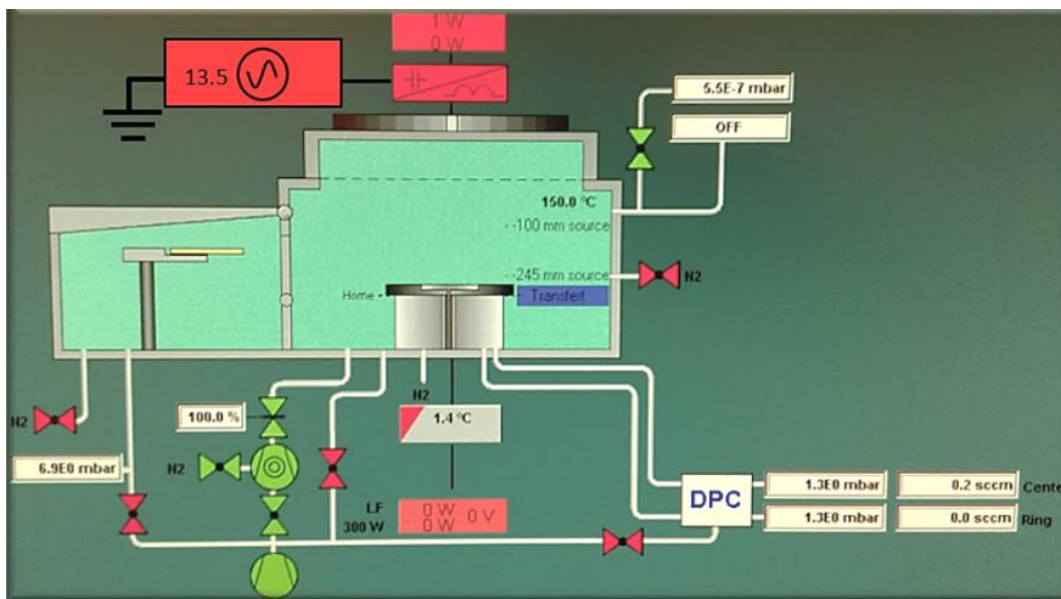

Figure 3.3 ICP RIE, MCI, SDU NanoSYD [26]

By using this method which employs the use of SF_6 and O_2 gasses to generate F* and O* radicals. O* is responsible to forming a passivation layer of SiOxFy, and F* is responsible for etching silicon, resulting in volatile products like SiFx. The passivation layer assisted by Oxygen is then removed partly by bombardment with ions. The remaining part of uncovered silicon is etched by F*. The reaction that takes place during etching is exothermic, and it reduces the possibility of resulting in a new passivation layer. Because SiOxFy is mainly a resultant of desorption during heating. At this point worth to mention that the reaction taking place in the plasma machine is as follow [27]:

$$Si + 4F = SiF_4 \qquad\qquad\qquad\qquad\qquad\qquad\qquad \text{Eq.1}$$

$$Si + 2O = SiO_2$$

$$SiO_2 + 4F = SiF_4 + O_2$$
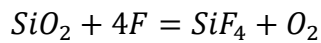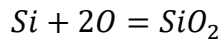
So, this reaction drives the etching/passivation competition mechanism which leads to the formation of random silicon microstructures. At this point to control the morphology of the bSi various RIE parameters should be adjusted. Starting from the gas composition, flow rate, system temperature, substrate bias, and RF power etc. contributors to different morphological changes. if a raise in O_2 flow rate is done, then a better deposition of the passivation layer can take place, on the other hand if the amount of SF_6 gas is increased than a more volatile reaction with Silicon can be seen. So while adjusting the coverage control, the passivation layer and density of nanostructures. by increasing the substrate bias during the RIE.

3.2 Control parameters for ICP RIE

Depending on the profile and thickness of Nanostructures as a function of the light reflectivity, there are several factors that should be controlled. In Inductively Coupled Plasma (ICP) machine to control the etching process, is more safe to change one variable at a time, because the difficulty of understanding the etching reaction increases.

- gas composition between SF6 and O2 [sccm]

- source power [W]

- chuck bias power [W]

- substrate temperature [°C]

- distance to the source [mm]

- etch time [min]

- pressure [mbar]

In my project work for all the variables given to change, only few of them I decided to change, as to monitor better the dynamic of the reaction. The black silicon layer, was created by only changing the gas composition of SF_6 and O_2, later was improved when the chuck bias power was activated. Gas composition plays a key role on Nanostructure's size and thickness. Going back to the plasma machine used Reactive Ion Etching Technique combined with Inductively Coupled Plasma was used [28]. Basically as we showed on the previous part ICP RIE it is a single machine, combining at least two gasses: the first one to generate radical species that can react with the silicon surface. The second one to passivate the etched surface. So in my case I use Sulfur hexafluoride Sf_6 to generate the radicals of Flouring (F') where they can generate volatile tetrafluoride radicals and Oxygen radicals generated by the same gas, able to passivate the silicon for uniform and deep texture size.

3.3 Solar cells

Nowadays, most common commercial type solar cells are Crystalline Si cell, Amorphous Si cell, and Thin Film cells. This variety of solar cells comes from the fact that different installation conditions and power demand from the user is required. And also different types of applications starting from industries factories, malls or end user have different demands on efficiency, performance, and cost. On the figure 3.7 monocrystalline, polycrystalline silicon solar cell are shown.

Monocrystalline
silicon solar cell

Polycrystalline
silicon solar cell
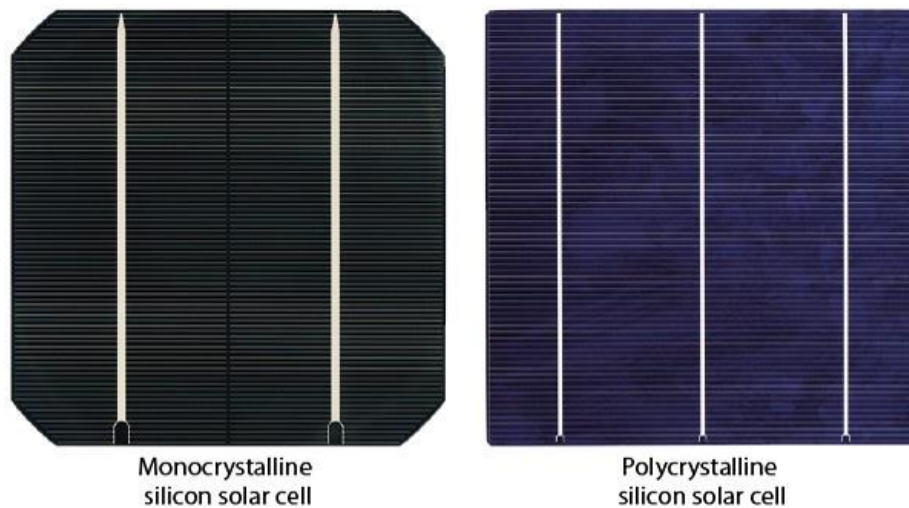
Figure 3.4 Typical mono- and polycrystalline silicon solar cells (left), and a commercial monocrystalline silicon solar cell (right) [29]

Monocrystalline solar cells can be found in a cylindrical shape, a characteristic that distinguishes them from polycrystalline solar cells. Despite these physical properties, they have some other distinguishable characteristic related in their microscale. That is mainly related to the crystal orientation and the mechanical properties of the silicon itself.

The construction principle for solar cells be it mono or polycrystalline cell, the layers composing it are arranged without any difference apart. In the figure 3.8 is shown the composition layer of a solar cell and the order they are combined to form the cell.
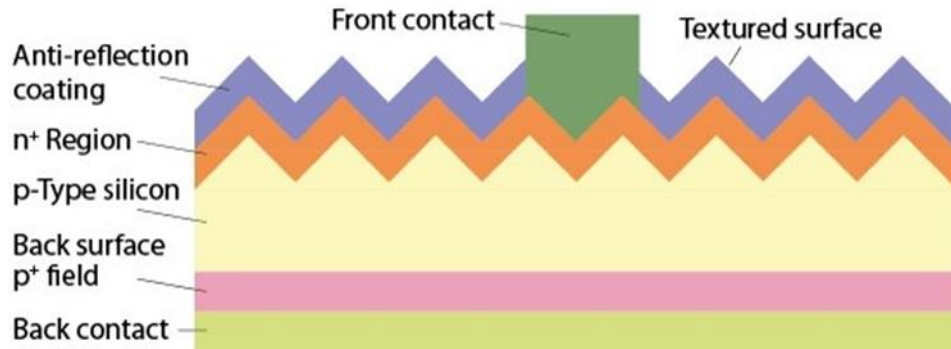

Figure 3.5 Compositing layers of a Silicon solar cell [18]

There are advantages and disadvantages per each type of solar cell that are related to power, efficiency and last but not least cost which is very important when it comes to a large scale of implementation of solar cells. Considering the impact that solar has over the other global energy sources the efficiency is close to hydropower and in the future tends to reach close to biomass. the graph below in figure 3.9 explains the current trend of solar with respect to other sources. [12]
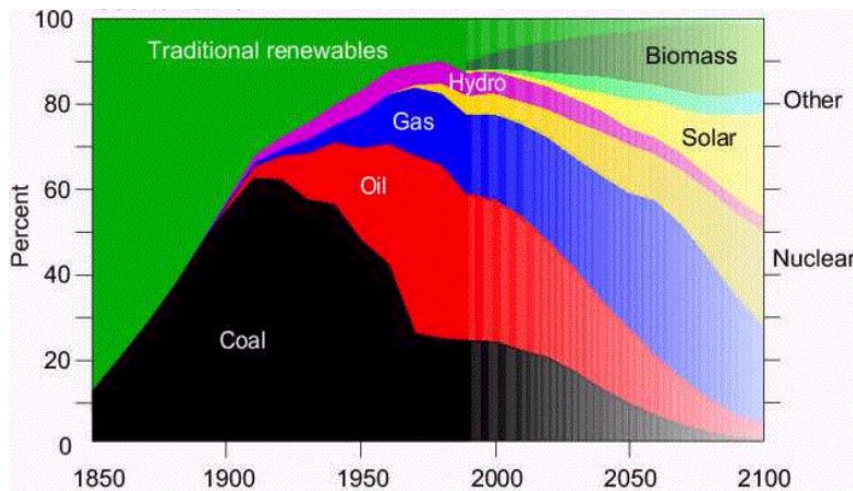
Figure 3.6 Renewable sources usage in percentage, Data World energy council [19].

3.3.1 Solar cells production

Considering the materials that are available today for solar cell production where among the most favorable ones are Silicon because of its abundance being the second abundant element on the earth with 28% after Oxygen. Hence being different form from the graph can be seen that to obtain different efficiency, each step on figure 3.10 has to be rigorously reviews, to lead in better quality of solar cells.
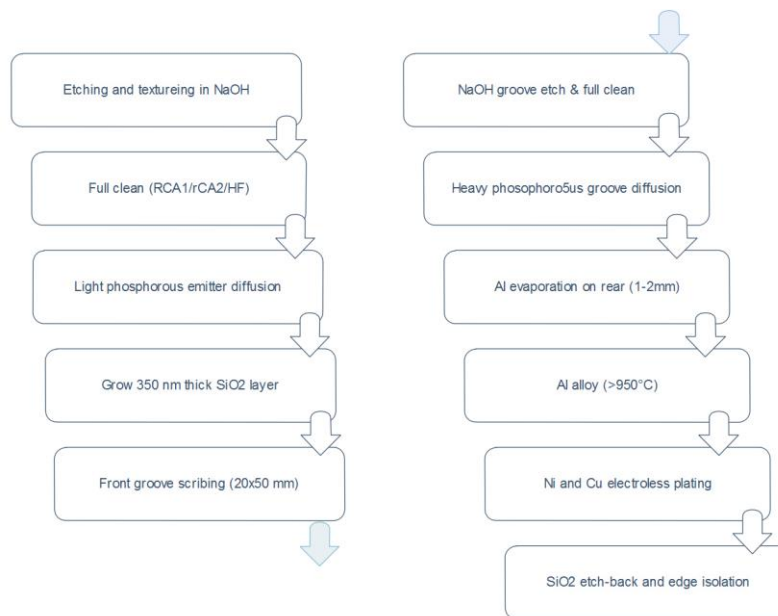

Figure 3.7 Convention Silicon solar cell production steps

Material, energy content and payback time are among the main factors influencing the solar cell production cost. An overview of these elements can be found in the table 9.2 added on appendences. And comparing this with the method that black silicon is produced some steps are shorter in time leading to a lower production cost. Now let's see what's the advantage of using the textured silicon and a normal planar silicon wafer which is illustrated on figure 10 where can see results for planar and textured silicon solar cells.

The materials used for antireflection coating the cost of the process will increase much more even though the efficiency will increase because the textured area will absorb more light. Different types of solar cells consider various criteria for production, starting from the type of coating, surface passivation, mask metallization, chemical resistance, temperature stability etc. For a review of common types of the solar cells in types look appendix table 9.4. the full table is reflected. So the major differences from a traditional PV production approach with say the IC/MEMS fabrication is in:

- Patterning
- Doping
- Contact formation
- Metallization
- Planarization.

So the thing that I want to do in order to create black silicon, starts simply with a pure silicon wafer inserted in a furnace where the combined dry and wet oxidation is used. After a thin layer of silicon dioxide. After wafer is moved out then etching of silicon in the ICPRIE machine starts. It is the effect of Ions Coupled into Plasma that can etch and create those textures, this is the primary reason why this machine is called Inductive Coupled Plasma Reactive Ion Etching machine (RIE). To create the idea how the structures, look like and a simple illustration on how ions etch through Silicon wafer to create black silicon.
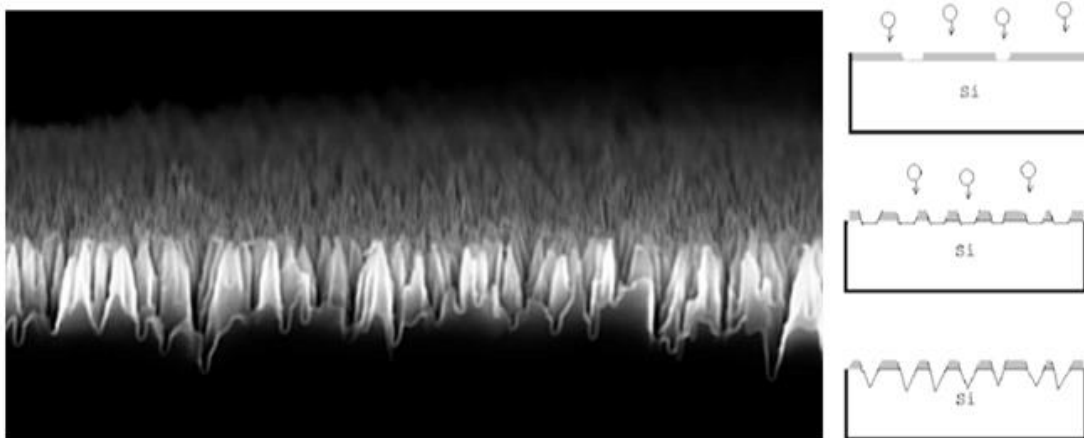

Figure 3.8 An example of a black silicon taken from SEM, etched in Plasma Reactive Ion Etching machine to create Black Silicon [18]

3.3.2 Black silicon in solar cells

In the figure 3.12 is shown a research comparison between treated and untreated silicon surfaces regarding absorbance and the result is as follow.
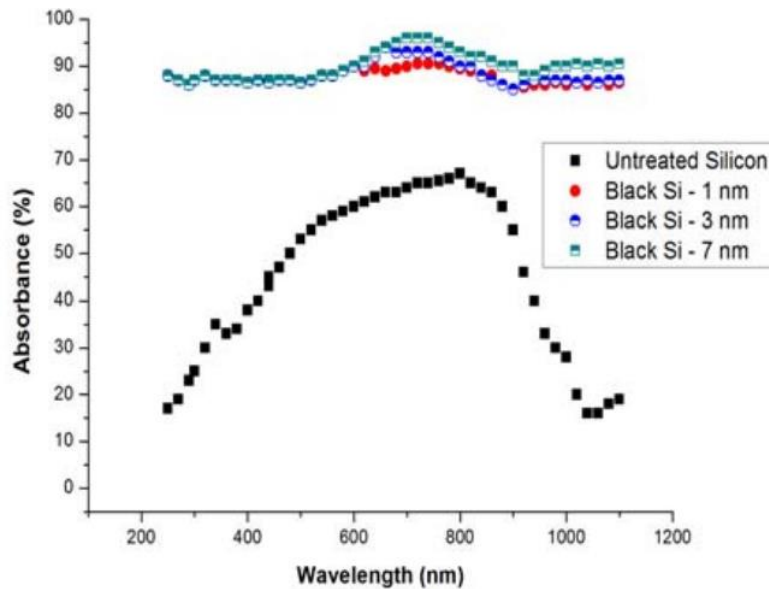

Figure 3.9 Normal incidence spectral absorbance from Black Silicon surface [18]

The 'black' curve represent untreated silicon, the blue curve is untreated polish silicon surface, and this is the part where companies that currently spend to create textures and make it absorb light. Conventionally textured silicon surface is the red one where big companies spend more money at What black silicon approach suggests is to minimize the production time onto creating the textures and replacing it with black silicon thereby shortening the steps and total processing time.
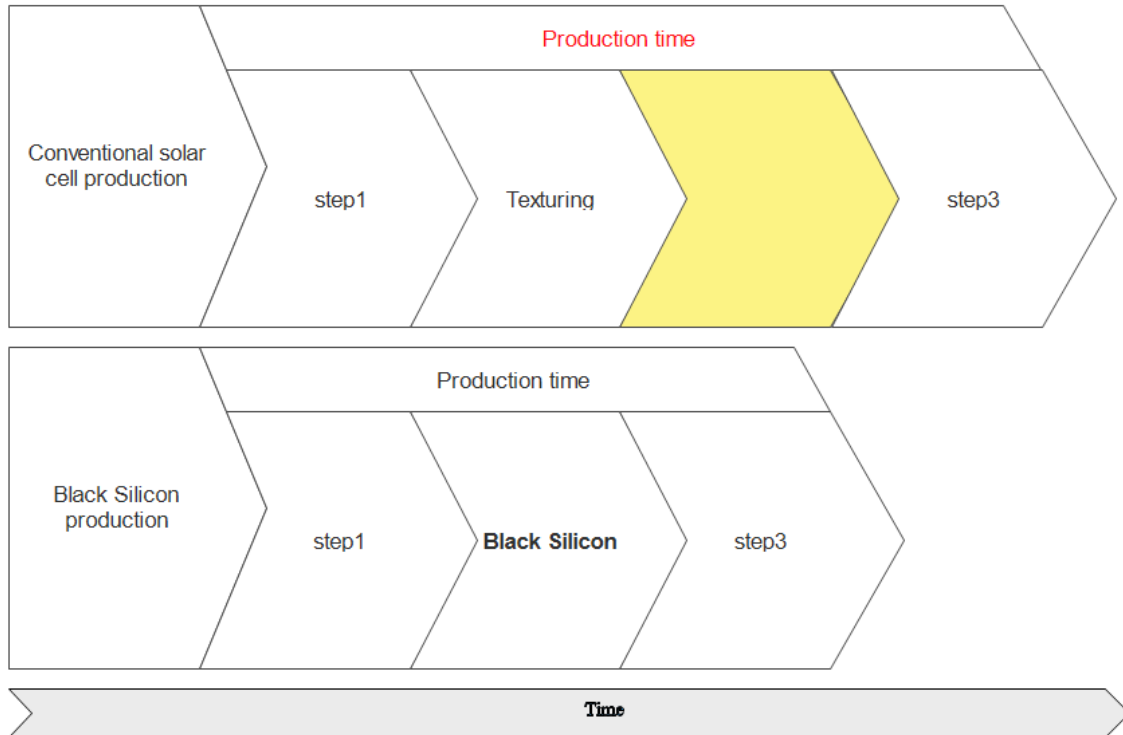
Figure 3.10 A simple block diagram over the production time of a conventional solar cell and that of a black silicon method

Referring to the Texturing as the main method to reduce the reflectance, is evident that with the conventional texturing the process of producing solar cells takes more time as shown in figure 3.13. And for Black-Silicon is different due to the etching process used called Ion bombardment.

Table 3.1 Black silicon solar method improvement [19]

	Black silicon	Conventional	Other research
Reduced cost	Yes	-	-
Higher efficiency	Yes	-	Yes
Less chemicals	Yes	-	-
Applicable	Yes	Yes	-

Though in the end It's all about cost efficiency, so if we look on table 3.1 either a reduction of the manufacturing cost or improving the efficiency would be the minimum solution.
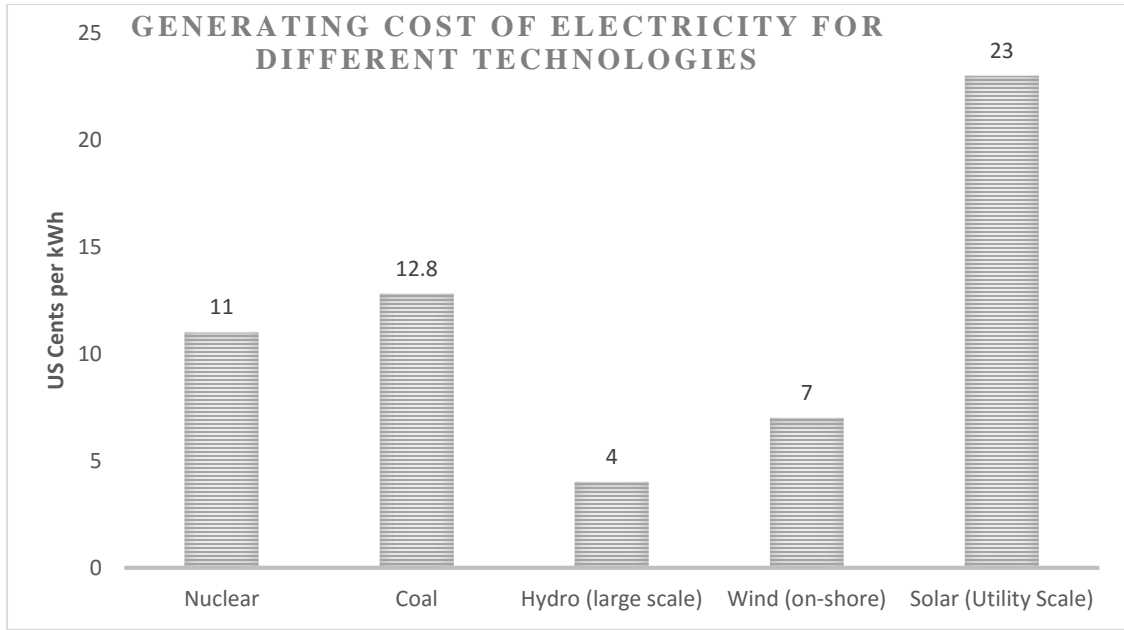
GENERATING COST OF ELECTRICITY FOR DIFFERENT TECHNOLOGIES

US Cents per kWh

- Nuclear: 11
- Coal: 12.8
- Hydro (large scale): 4
- Wind (on-shore): 7
- Solar (Utility Scale): 23

Figure 3.11 Sources: Nuclear, Coal: Parsons Brinckerhoff" Powering the Nation" [24]

Reduced manufacturing costs are the most important thing where if looking at the solar energy is still too high the cost so to improve the efficiency and reduce the manufacturing cost or both. To replace the manufacturing process and reduce the cost per watt production. On the table 3.4 the production time and cost is given, for conventional texturing used as an antireflective layer and the black silicon. From the data given we can see that conventional texturing takes 12% more time, and 10% higher in cost than black silicon.

In appendence 9.1 the table about the energy usage in W/kg of the materials is shown with respect to the cost of the materials, in the final stage. Though particularly on the figure 3.14 the cost in US cents for the market is given, according the type of energy source utilized.

Table 3.2 production time and cost production of Black Silicon [19]

	Time min (% of total)	Cost % of total
Conventional Texturing	40 (14 %)	13 %
Black Silicon	4 (2 %)	3 %
Reduction, total in manufacturing	**12%**	**10%**

comparing the conventional texturing with black silicon the estimated cost reduction is about 10%. Referring the table 3.2 the absorbance and cost are main factors for applying this method. But the production of black silicon will not be only as an advantage for the usability side. Instead, there are also some mechanical properties like hydrophobicity where in the case of dirt of foreign particles that might limit the efficiency of solar cells. A wash with liquid would be like a 'perfect' cleaner for its surface since the dust particles will be washed away by surface tension forces. Another mechanical property is the ability to withstand the expansion. Where being 'black' means that the light will be absorbed and eventually create a higher possibility to absorb more light therefore leading to good efficiency as shown in the figure 3.15.
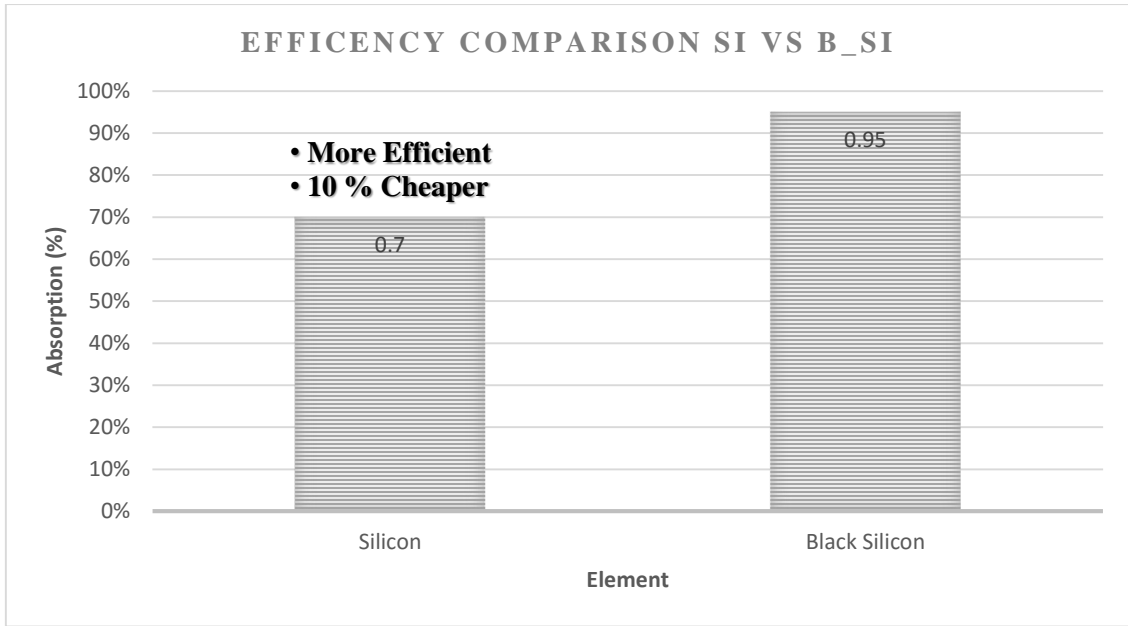
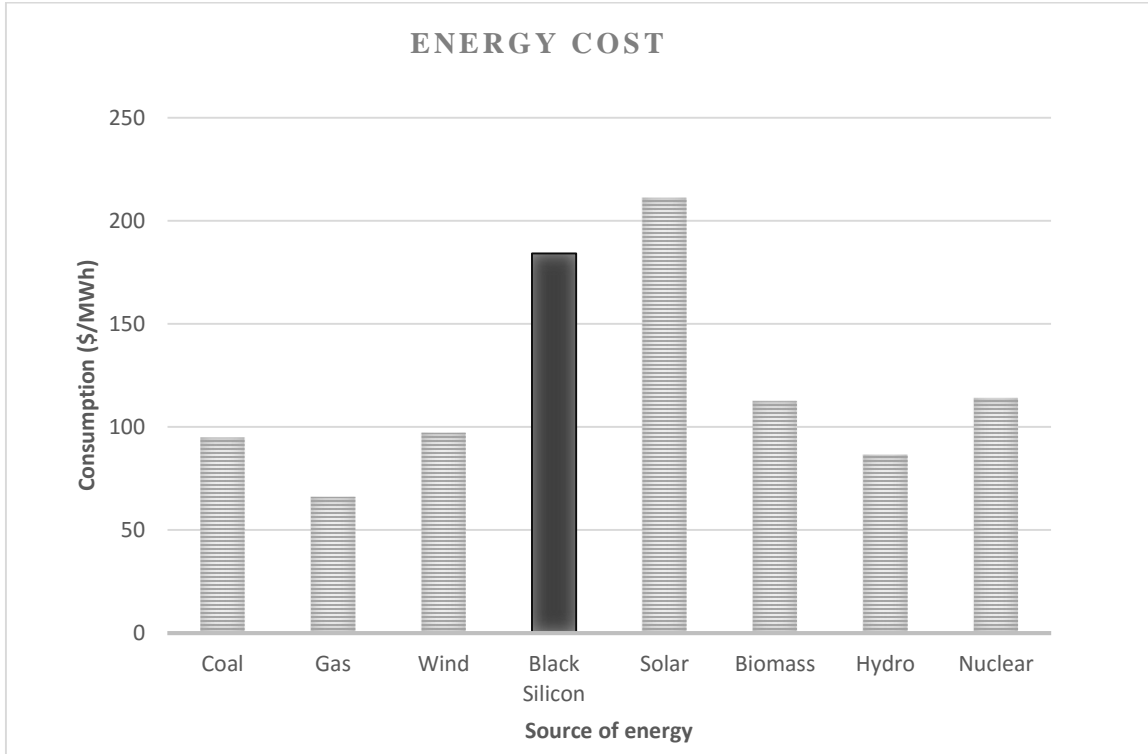Figure 3.12 efficiency increase introducing Black Silicon [7]

Table 3.3 Black Silicon on solar cells among other energy sources [30]

4 DEVELOPMENT OF BLACK SILICON

The samples made ready for the etching process in ICP RIE machine were placed in the wafer holder using a thermal glue. That is required to make sure that the sample will have good conductivity with chuck bias[3]. Necessary when etching with different power level in chuck. The samples were cleaned and collected before starting the etching process in ICP RIE machine and loading the wafer shown in figure 4.1.
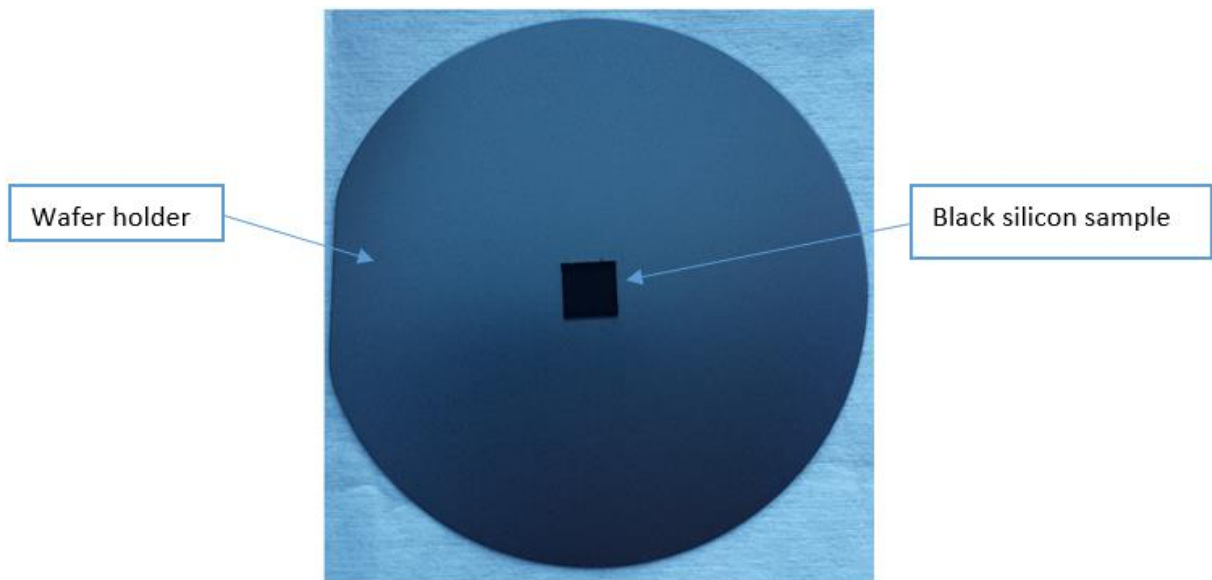

Figure 4.1 wafer holder and sample in the middle

A full wafer can be treated in the ICP RIE machine. Though due to many variables in the process, more convenient was to cut portions of raw silicon and have many of them ready for different etching parameters.

---

[3] threshold power for charging the sample (silicon wafer) applied on a movable platform.

4.1 Silicon Etching

For the silicon etching process the gas mixture and the recipe was executed in the machine immediately would lock the sample in and put into the reaction chamber, there on the plasma cloud the etching process took place. For silicon the etching started when the O2 was in contact with SF6 gas in a different ratio. So for the first recipe a ratio of 90 sccm of Sf_6 and 100 sccm of O_2 was used. After its execution the etching process run for 5 minutes in a position of 200 mm from the reactor, in the source of the plasma. Worth mention here that during the silicon etching process for treating the samples, the temperature set for the machine was -20 °C. Because the temperature in the machine during the plasma conditions it high and the chuck, which holds the wafer has to compensate by cooling it during the process. So the parameter that were set for the plasma machine during etching process were as follow:

Pressure:1.3 e -4

Chuck heating: 200mm

Center He regulation: 6.6 sccm; pressure 1.01e1 mbar
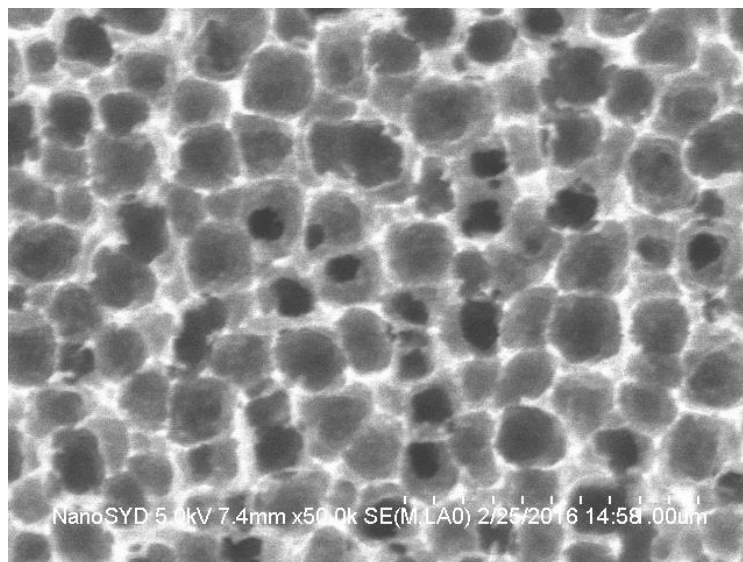
Ring He regulation: 10.6 sccm; pressure 1.01e1 mbar

Figure 4.2 SEM top view of the sample after ICP RIE, MCI NanoSYD

4.2 The 'black silicon' method

The black silicon can be attained using different methods where etching was one of them, used in this work. In this context the reason called black silicon method it is related to one step process which is simple and one-time etching. So this method can save time and is simple to apply once the parameters are set right. Which basically was our task when using the plasma machine the ICP RIE. Because of the reaction complexity that happens during etching the control of the gratings shapes will vary, which it is a variable to control the shape of the grating will define the quality of 'black silicon' Though using the Florine-based plasma machine and the black silicon method, to etch which creates a favorable process for the substrate not damaging it (electronics) or eroding the mask. In the black silicon method, the profile of the trenches can be changed by altering the plasma chemistry like power, pressure, gas flow and ratio etc.

Considering the RIE machine specifically, in such plasma SF6 produces F+ radicals for the chemical etching and O2 creates o+ radicals for Si passivation in correspondence with SiOxFy and CHF3 as the source for CFx+ While the etching process for creating the Nano textures as a combination rate of SiF4 and O2 the question that naturally can be done is can I take the values from a successful know etching process and transfer them for our process? At this point a simple and short answer can take an answer with no. Because same recipe on different devices may produce different results even when the machine is identical it depends on such profiles as power, pressure and gas flow. The fact of black silicon and its rate of success is related to the vertical profile regime this means that to get close to an almost vertical wall, in order to name it the 'black silicon method' [16].

4.3 Quality factors

To estimate the efficiency of black silicon fabrication and the limiting factors, that confine the geometry and therefore affect the light trapping surfaces. Trying to use a simple analytical model, which was the gas ratio approximation in respect to the size of the structures and the reflection rate. The approximation was done using the ratio of Sf_6/O_2 by changing it from 0.9 to 0.7 with 0.5 scales to test the quality of black silicon and later analyze the shape of the Nanostructures. This was the start point to control the quality of the structures for preparing the recipes, though not quality factors. After several steps of trying the process in the machine, practically could control the quality of the samples in two stages. The first one was the preparation procedure for putting the samples into the machine.

The second quality step was related to the placement of the sample into the holder and the He gas leakage on the wafer. So to make sure that the samples carefully and not contaminating them precise timing in the chemical room was used, special tweezers for holding the samples, well-washed beaker and the same amount of cleaning chemical for each sample. And the last but not least step to control before running the machine was the sample gluing into the wafer holder, which had to be done correctly laying it flat with the holder and making sure to have a good thermal contact to see the gaps (if any) between the sample holder and the sample itself. The last quality steps were related to the machine for any gas leakage like He gas around the wafer and any possible problem with the pressure in the reaction room. Since any of these factors could affect the etching directionality and the uniformity. So for each step missing the process was repeated again.

4.4 Operation with tools

For using the tools, provided with the right assistance from the cleanroom staff and also the manuals provided from university's website Nanosyd.dk. The machines ready to operate were ICP RIE, SEM, Spectrometer etc. where the instruction to use them were given verbally from the cleanroom staff and partly some information was taken from the manual especially for the SEM machine to understand how the electron beam works for achieving the best images with high magnification.

Figure 4.3 Hitachi S4800 [31]

Here on figure 4.3 is shown a similar model of the Scanning Electron Microscope used in the cleanroom facility at SDU, S-4800. Though at this picture is shown clearly the size and space it takes to run this equipment.

4.4.1 Scanning Electron Microscopy

Using it precise imaging methods high details of the sample were taken by analyzing it from two different perspectives one from the top view and the other from a side view where the second one was by cutting the sample in two pieces and analyzing one piece from the sample in the same place where the cut was applied. So with the top view the morphology of the Nanostructures was visible. For the side view, the dimensions of the trenches and their profiles were taken.
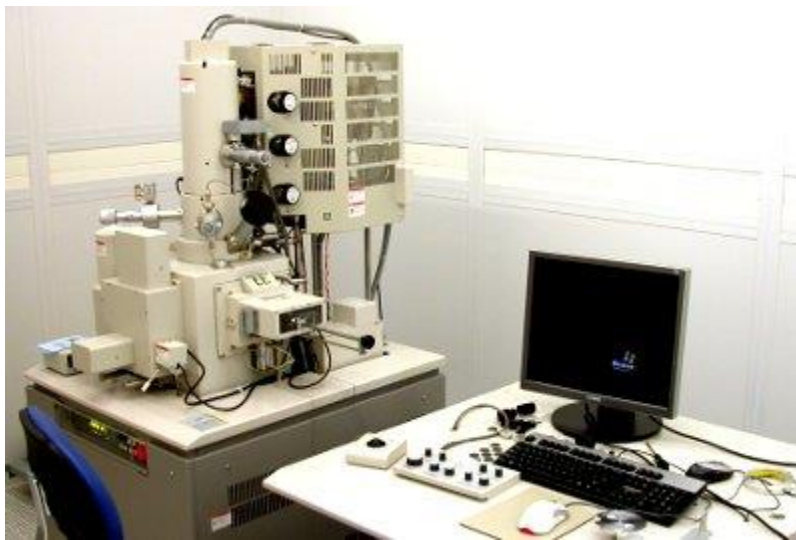
Figure 4.4 Scanning electron microscope, MCI NanoSYD [32]

In Figure 4.5 the Scanning Electron Microscope running at SDU is shown. The model installed is S-4800 it is used to operate not only to take images but also for the Electron Beam Lithography. As a tool to transfer the patterns in the substrate more accurately through electron beam.
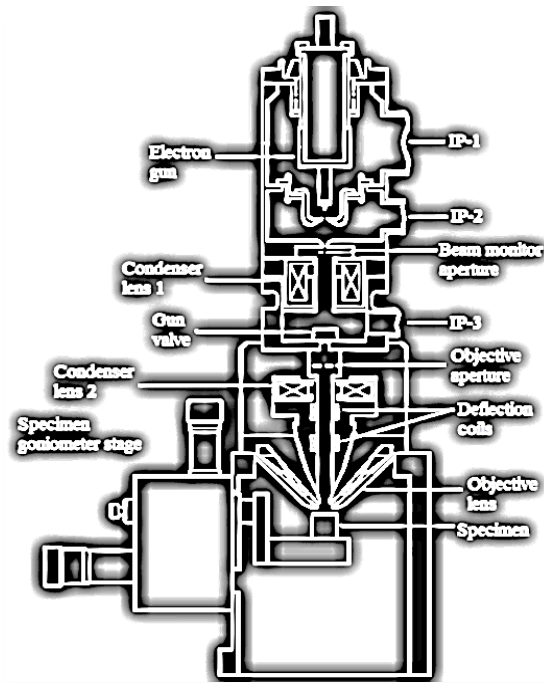
Figure 4.5 SEM primer [33]

A look inside the SEM as on figure 4.6, will give us some information about the source (electron gun), ted condenser, microscope column, specimen chamber, and vacuum system that are on the left. The computer, monitor, and many of the instrument controls are placed on the right. As an operator one will need to understand what is happening inside the "black box" (microscope column and specimen chamber). Hence when an instrument control is done all the changes of the parameters are shown in the monitor, starting from the beam power, zoom magnitude, brightness level etc.

Thus to make it simple to understand, the electron beam accelerates down the column; through a series of lenses that are able to control electron beam diameter as well as the focus the beam on the specimen. Then a series of apertures allow the beam to pass through, where this aperture can control the properties of the electron beam. Control for the orientation like rotation, tilt is controlled. So an area responsible for the specimen/ beam interaction generates various types of signals. which can be detected and further processed into producing an image or spectra.

4.4.2 ICP RIE

These tools are used to etch the surfaces of the substrates by using dense plasma which is produced using high currents rated at a high frequency. Having a good control of the species is essential for this process. The method on which plasma machine can etch and the accuracy achieved to create the sidewalls is descent and that it was done using the cryogenic sidewall passivation method. Which makes use of thick photoresist layers and Silicon etchants like SF_6 and O_2 at low temperatures. That is to minimize the problems related to layer structures and built-in stress and/or thermal expansion coefficients.

The etching process in ICPRIE combines two types of plasma machines. Inductively Coupled Plasma (ICP) which is basically like a transformer coupled plasma (TCP) [9] and is considered a type of plasma source where the energy is supplied by electric currents produced by the electromagnetic induction, with time-varying magnetic fields. An example regarding the basics of both types is shown in figure 3.1.
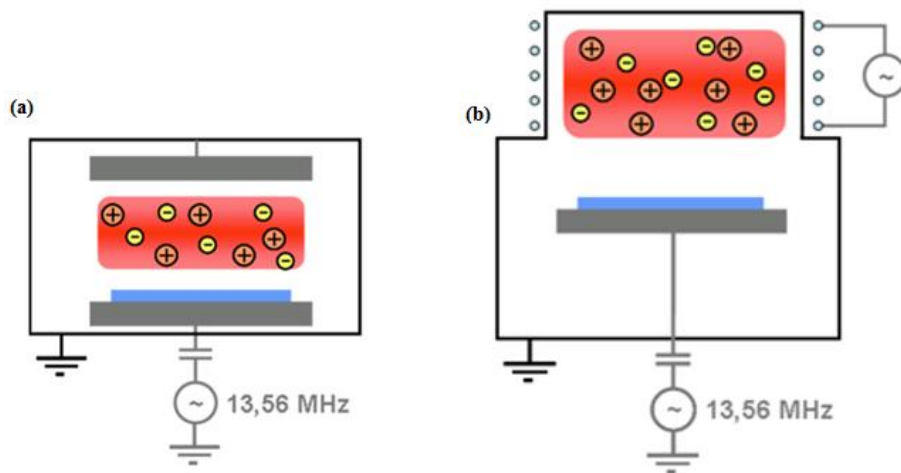

Figure 4.6 (a)ICP , (b) RIE [25]

Whereas the Reactive Ion Etching which is shown in figure 3.1 (b). It is another type of plasma etching with different characteristics, it uses the reactive plasma to remove the material in the substrate.

The conditions under which the plasma is generated are those of a low vacuum pressure and an electromagnetic field. Which then favors for the ions to be formed at plasma cloud attack the surface of the specimen or sample thus, reacting with it. The machine used in the cleanroom facility for the work is ICP RIE that combines both methods and properties mentioned from two previous types of machines. A basic figure showing its working principle it is shown below in figure 3.2

Figure 4.7 ICP RIE Cleanroom NanoSYD, Alcatel AMS110 SE

On the figure 3.2 the ICP RIE plasma machine is shown, the core part of this machine is composed from left module which is the place where the plasma is generated, and the right part where the vacuum pump and the valves or pressure is controlled. This machine is located in so called the grey area[4] where the cleanliness of the environment is orders of magnitude less than inside the cleanroom environment. The cleanroom at SDU is a 100 class cleanroom according to ISO 5 standards.

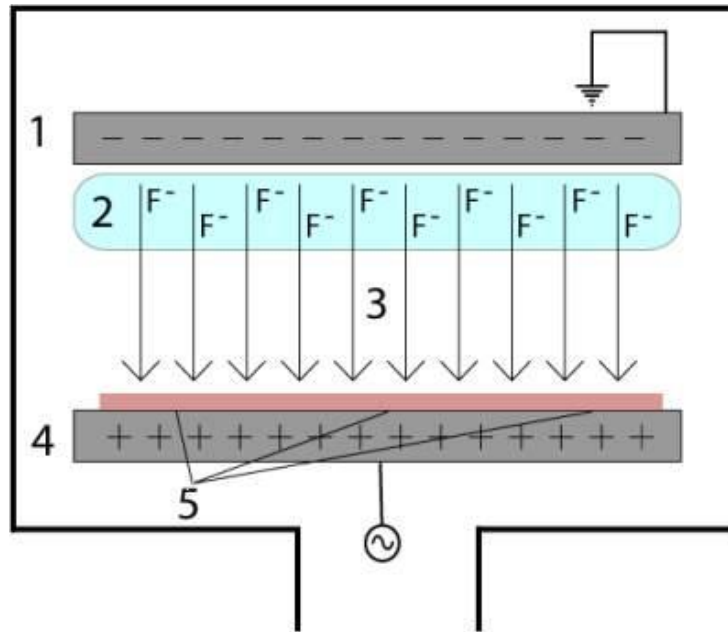[4] The area where the interim space between the surroundings and the white area meet.

Figure 4.8 A diagram of a common RIE setup [26]

The steps into which the plasma machine etches the material on the specimen may it be ICP, RIE or combined as in our machine, three main stages can be distinguished. The influx of reactants that might be SF_6, O_2, CF_4 etc. the reaction stage where the specimens created from plasma condition hit the sample end etch it. And the third stage is that of a removing the byproducts etched away and removed from the plasma machine.

The plasma machine shown on the figure 3.3 represents the real setup of the machine used on the Cleanroom environment at SDU. From the picture one can see the generator for the high frequency operating at 13.56 MHZ, where the power for the chuck bias is applied that has an advantage for this machine, which makes the etching process more fast and efficient.

4.4.3 Results and discussions

So what we saw from the images taken from SEM and the characterization with microscopy and analysis with ImageJ[5] we could see that there was a regularity regarding hole density and their dimensions to produce the minimum reflectivity possible for the solar cells. And the main factors that were affecting the size holes was the gas Sf_6 hitting the substrate and O_2. The next factor affecting the holes was the chuck bias as well based on the images acquired from the samples that were produced with 2W 4W 6W we could see that they were deeper on the holes and the edges were sharper. And looking at their dimensions and comparing with the images we took just by changing the gas ratio for the same scale we can see that the size of the holes in the second case is bigger and the frequency of those holes in the substrate is lower, meaning less dense.

---

[5] ImageJ it is a public domain, Java-based image processing program

5 EQUIPMENT AND METHODS

During the work for fabricating the silicon handling the samples, inspecting them and acquiring the data a set of devices was used. For preparing the silicon samples for the next etching process the 'yellow room' got utilized for the ICP RIE to etch the samples by varying only the gas ratio between Sf_6 and O_2 and keeping the other parameters constant. Then the next stage started with the Scanning Electron Microscopy (SEM). The size of the structures, shapes, position and density. After taking images with SEM, the reflectivity test and absorption rate was measured. The last test was to measure the angle for hydrophobicity and hydrophilic, where based on water contact angle the results were combined to confirm the images taken from SEM.

The SEM, ICP RIE were not the only equipment's used during this work, in the last stage we used the Water Contact Angle as well, to measure the hydrophobicity of the black silicon surface, also for samples treated with Bosch. In this chapter part 5.6 more details will be shown, on how it is setup and the results we got from the test. Also for the reflectivity test another setup was built to measure the response of the sample in different wavelength. That was generated from the spectrometer to check how the reflectivity of the sample (s) changes when the different Electromagnetic waves hit it.

5.1 Black Silicon study

Before starting the work in the cleanroom, the work steps were scheduled in stages until the final step aiming to achieve good results using timewise the facility. So, at first, the sample of black silicon from known recipes studied from literature [16]. Then after each stage, the best sample(s) chosen by inspecting the images taken from Scanning Electron Microscope (SEM) and reflectivity test.

In the first stage of this project black silicon was fabricated on a clean silicon wafer through plasma machine with the aim to check the difference in microstructural level(s) and the black silicon behavior on the surface of a raw silicon wafer. The first samples were created by changing the gas ratio of SF_6 and O_2 in ICP RIE machine, using reference values from previous researches regarding black silicon [14]. The other samples fabricated afterward were generated with a ratio close to the first one. And the results were taken as a feedback for the next recipe
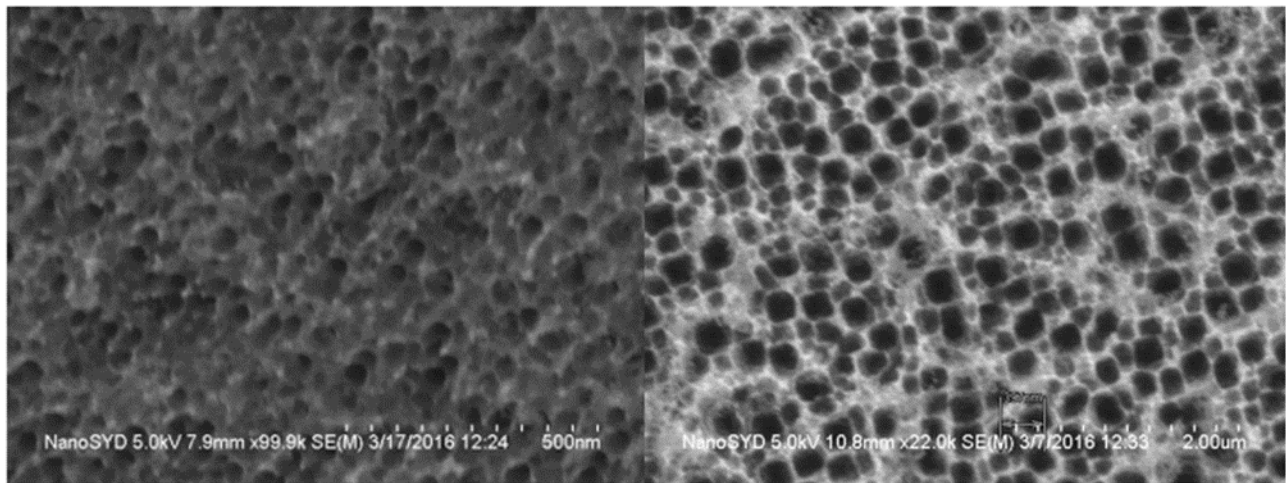

Figure 5.1 left, poor black silicon sample right, descent sample, MCI NanoSYD

The work overview for the black silicon study stage are shown on the figure and per each stage notes on the parameters that did not work correctly were saved.
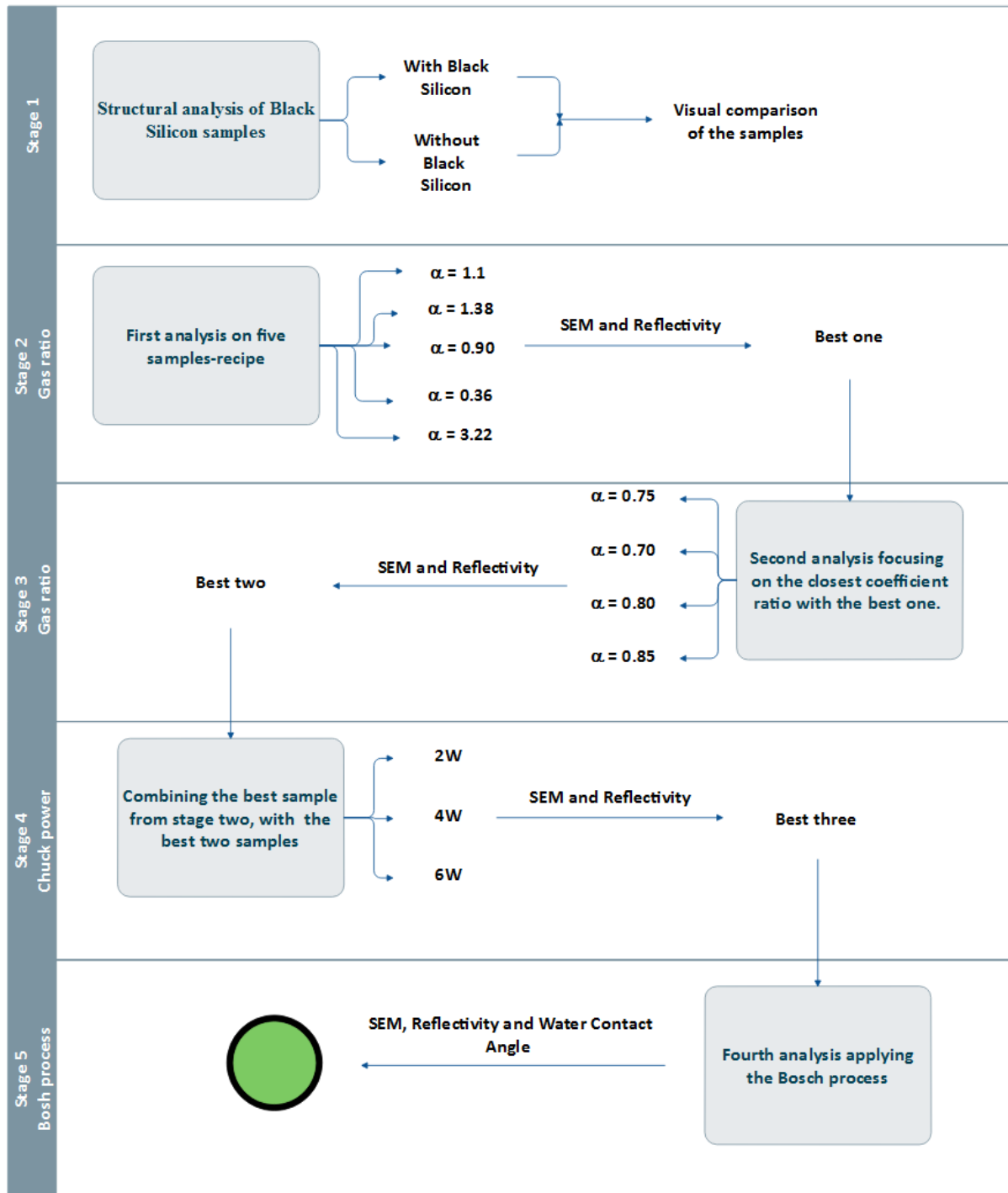

Figure 5.2 Work overview during black silicon study stages

In the early steps of black silicon characterization, was chosen to select the best samples looking at best SEM images and later on by reflectivity measure). The criteria used for SEM was the regularity of the microstructures, size and density of the holes, which are the main variables for the light scattering inside. For the next stages were added, as selection criteria, reflectivity measurements. These made the selection process between the samples easier. Important to mention here is that during the process, to create good samples, was necessary to re-do some of them because of contamination or problems in thermal conductivity in the ICP RIE machine; to prevent these problems cleaned samples from a raw silicon sample cut were used. After the cut of the samples, these were put in three different beakers filled with acetone, isopropanol, and distilled water. in the process was: each solution for three minutes respectively and then dry by blowing air onto the samples surface. The samples were after putting into the ICP-RIE and studied. The results and problems faced in each step will be presented later in the following chapters.

The analysis will start from the test samples made to understand the properties of black silicon and measure the feature sizes, for later comparison with other samples. Then per each stage the final sample (s) result was stored and recombined with later stages, to derive good quality samples from the original recipe. Hence the pictures during each part will help understand the 'surface nature' of each sample produced with a certain recipe, consisting of gas and power combination. As the main variables of this process.

5.2 First stage

In the first stage, the structural analysis of the black silicon and acquired the images from Scanning Electron Microscope (SEM) to characterize the samples. Then the process was noted regarding the geometrical shape and size of the microstructures created on top of the silicon sample. This was to understand how the ratio of the gasses respectively SF_6 and O_2 affect the geometry of the microstructures after the etching process takes place. The process, started in plasma machine where only one variable was set as a start, the ratio between Sulphur fluoride and Oxygen, combined in a recipe suitable to create black silicon from the previous research work done for it [24]. When the samples were ready for the plasma machine, the visual inspection from SEM took place. The images acquired are shown in figure 5.3.
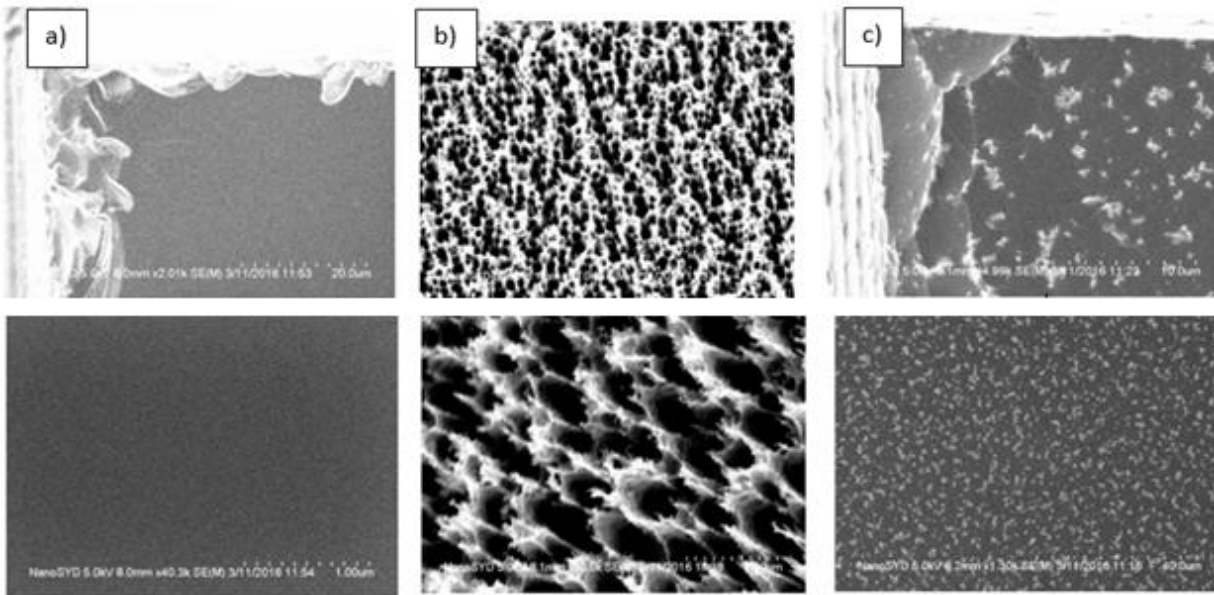

Figure 5.3 left untreated silicon sample, middle treated black silicon sample, poorly treated sample MCI NanoSYD

Only the recipe (b) with gas ratio SF6/O2-100/90 resulted in black silicon the other recipes with two times more SF6 or O2 gave very poor results into creating a black silicon as in case of (c) which is quite close to the case of untreated samples shown in figure (a).

5.3 Second stage

For the second stage, five samples were prepared and analyzed according to the steps planned on the working schedule. One out of five samples was saved as the next recipe for the next stage. Then the reflectivity test took place for the rest of the samples and in the end the results only from the best one were compared it for the later stages. The reason of creating five samples and select the best one, was to find what is the trend of the structures when the ratio of gasses changes in an exponential function. I did that by starting from the previous best recipe with α=0.9 and then changing the ratio of gasses by inversely increasing or decreasing the amount of gasses close to an exponential law as shown in table 4.4 with the aim to tune the recipes faster. The results I got from the SEM images of all the samples treated with gas ratios as in table 5.1

Table 5.1 Gas ratios derived from the recipe with gas ratio α=0.9

Alpha SF_6/O_2	Sf_6	O_2	O2 trend	SF6 trend
1.1	100	90	(reference)	(reference)
1.38	110	80	-10	+10
0.90	90	100	+20	-20
0.36	50	140	+40	-40
3.22	145	45	-95	+95

The SEM images from this stage are shown in part 5.3.1 where top and side view of five samples, along with reflectivity data will be shown.
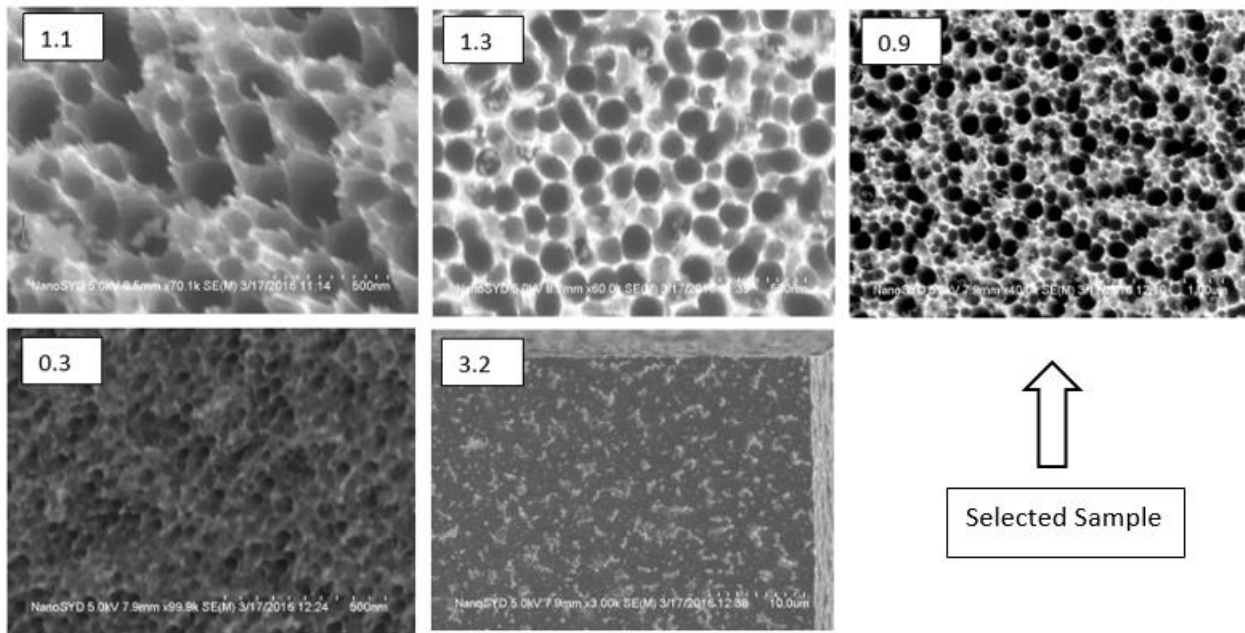
5.3.1 SEM Images

Figure 5.4 Top view images of the samples derived from the main recipe, MCI, NanoSYD

From the top view images of SEM, the best samples with ratio α=0.9 are more regular structures and the shape of the holes is more circular. After inspecting the top view images, according to the criteria mentioned regarding regularity, size, and shape, the same was done for the side view images taken after cutting the sample with a diamond tip and the sample with α=0.9. proved to be the best one from the regularity of the structures for more details below on figure 4.5 are shown the side view images for all five samples.
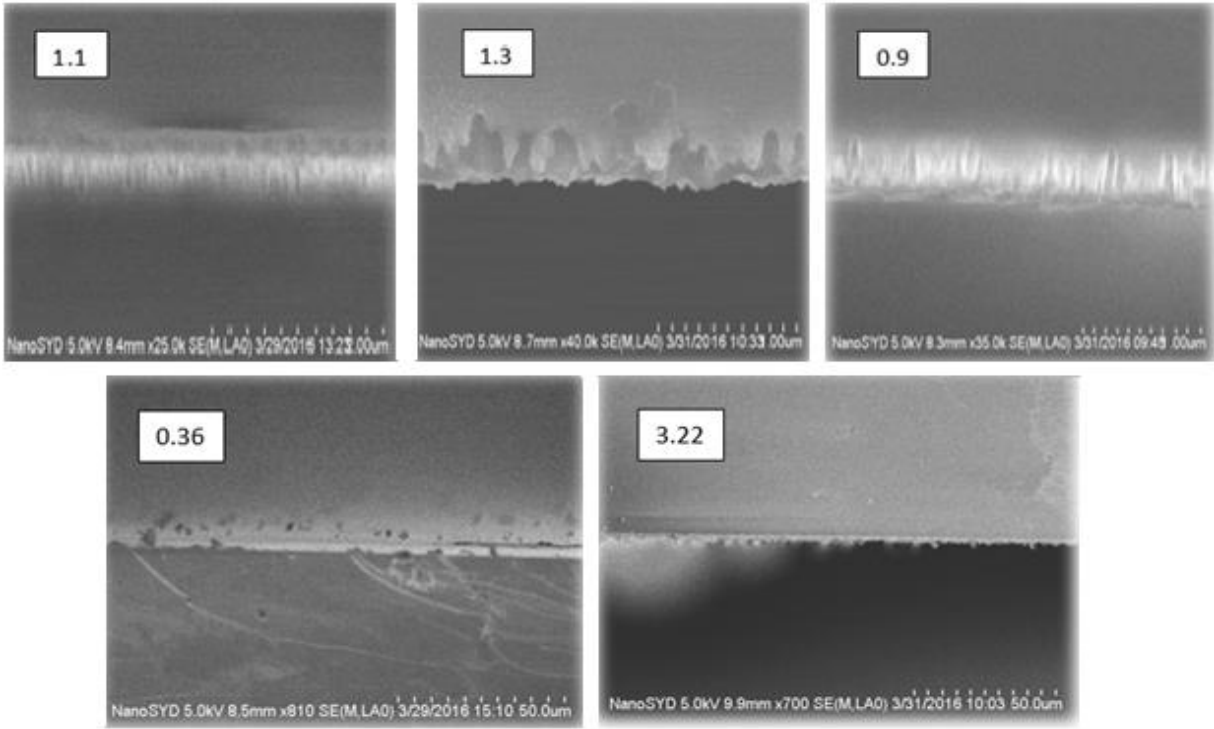
Figure 5.5 SEM images from the side view, MCI NanoSYD

For the side images, of the black silicon the sample with α=0.9 had good Nanostructures confirmed from SEM, it showed to be the best among others, and for further inspection as to understand the shape of pillars, size and relationship to the light absorption rate. ImageJ was used to measure the dimensions of the pillars. Below the results.

Trenches No.	Height (nm)	Width (nm)
1	3.189	1.089
2	3.236	1.007
3	3.424	1.124
4	3.444	1.299
5	3.061	0.943
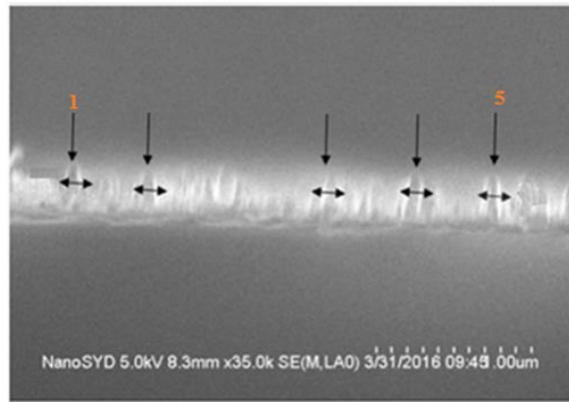
Figure 5.6 Geometrical size of the best sample α=0.9, MCI NanoSYD

5.3.2 Reflectivity

Figure 5.7 Reflectivity measurement setup

After SEM analysis was the reflectivity measurement. That gave a numerical approach how to improve the light absorption rate.
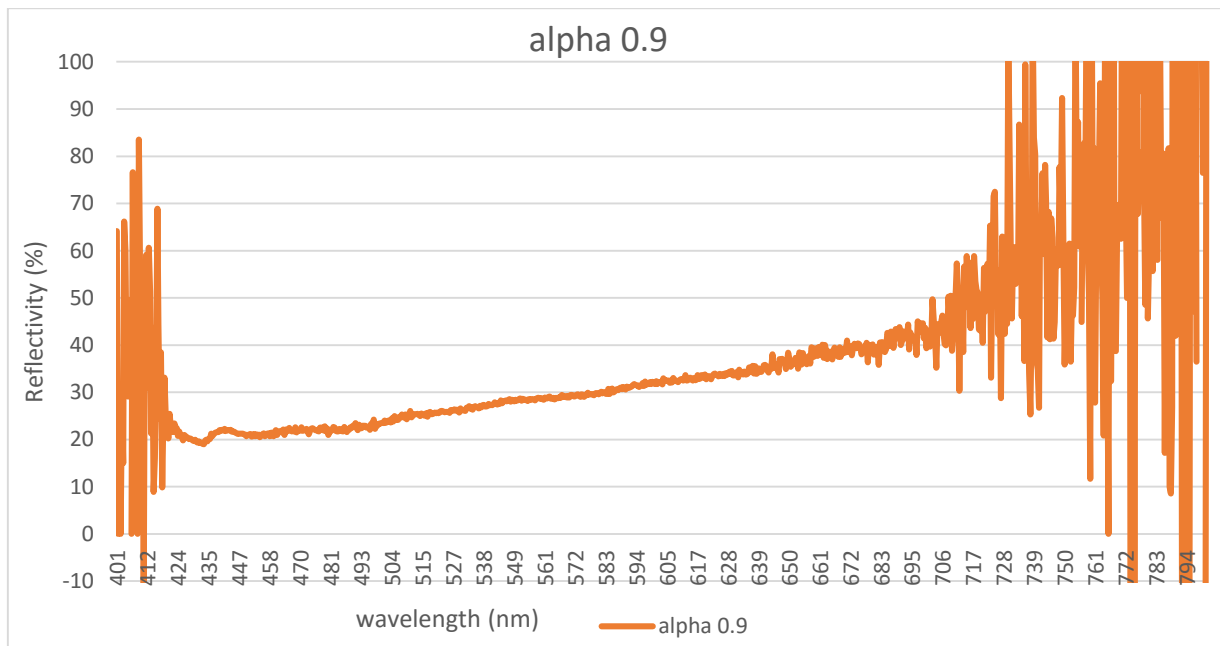

Figure 5.8 Reflectivity for the best sample

5.4 Third stage

On the third stage four new samples were derived from the best one (α=0.9), during first selection. Then from this recipe two best samples got extracted, for this case the SEM and reflectivity test was done. A simple procedure is shown on the figure 5.9
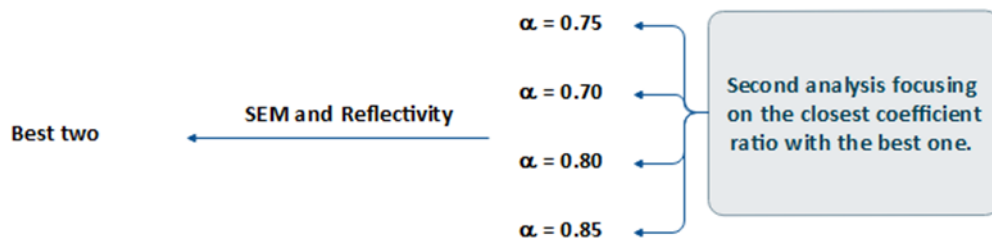

Figure 5.9 Third stage tasks for selecting the best sample

Ratio SF$_6$/O$_2$	SF$_6$	O$_2$	
0.75	81.4	108.6	**Derived from recipes**
0.70	78.2	111.8	**With α**
0.80	84.4	105.6	**1.1 - 0.9**
0.85	87.3	102.7	

Table 5.2 Gas ratios for the derived recipes

In the images below, is possible to look at the results given by the SEM inspection of the top view and side view after applying the derived recipes into the ICP RIE machine.
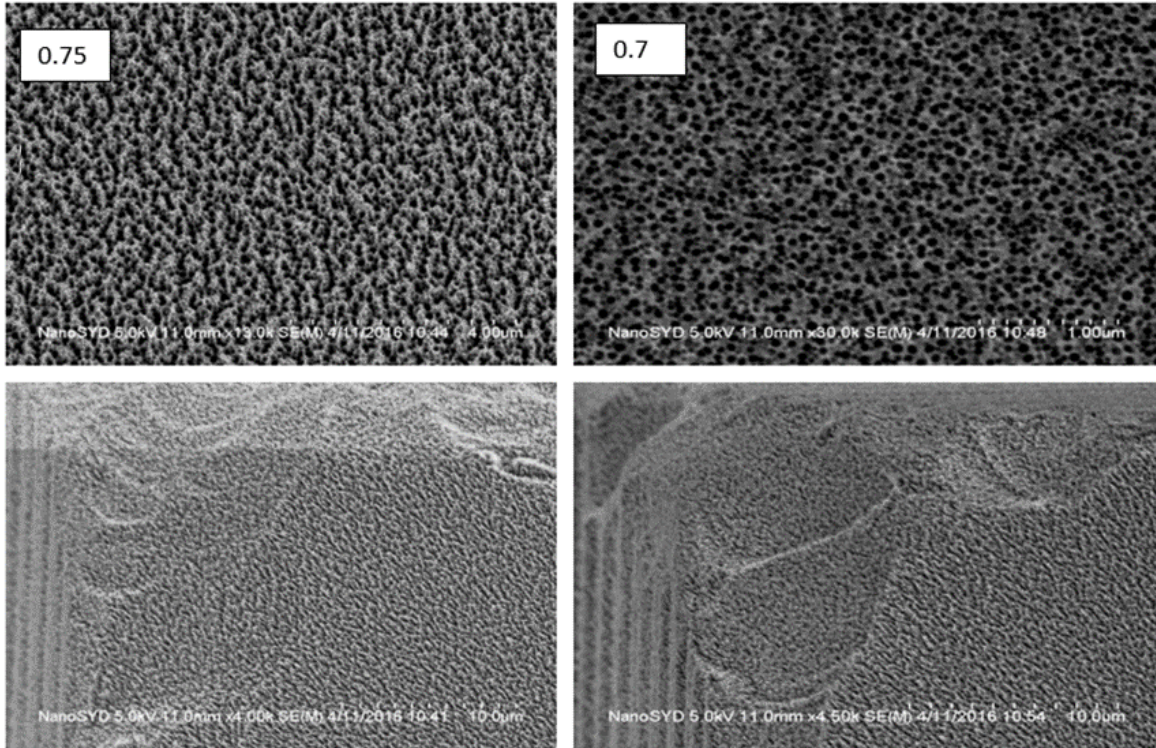
Figure 5.10 SEM images top view images, MCI NanoSYD

From the SEM image acquired is evident that in both cases the microstructure is created (between the 'holes') are spread across the sample with the same density, and their size is roughly the same in all the regions. Though for sample with α=0.75 the structures are more regular and deep, whereas on the right image of the sample with α=0.7 then the microstructures are poorer and not sharp.

To compare with the other two samples out of four created another set of SEM images was taken figure 5.11 then send them for the reflectivity test, where both data combined from SEM and reflectivity could give a better result which sample is the best.
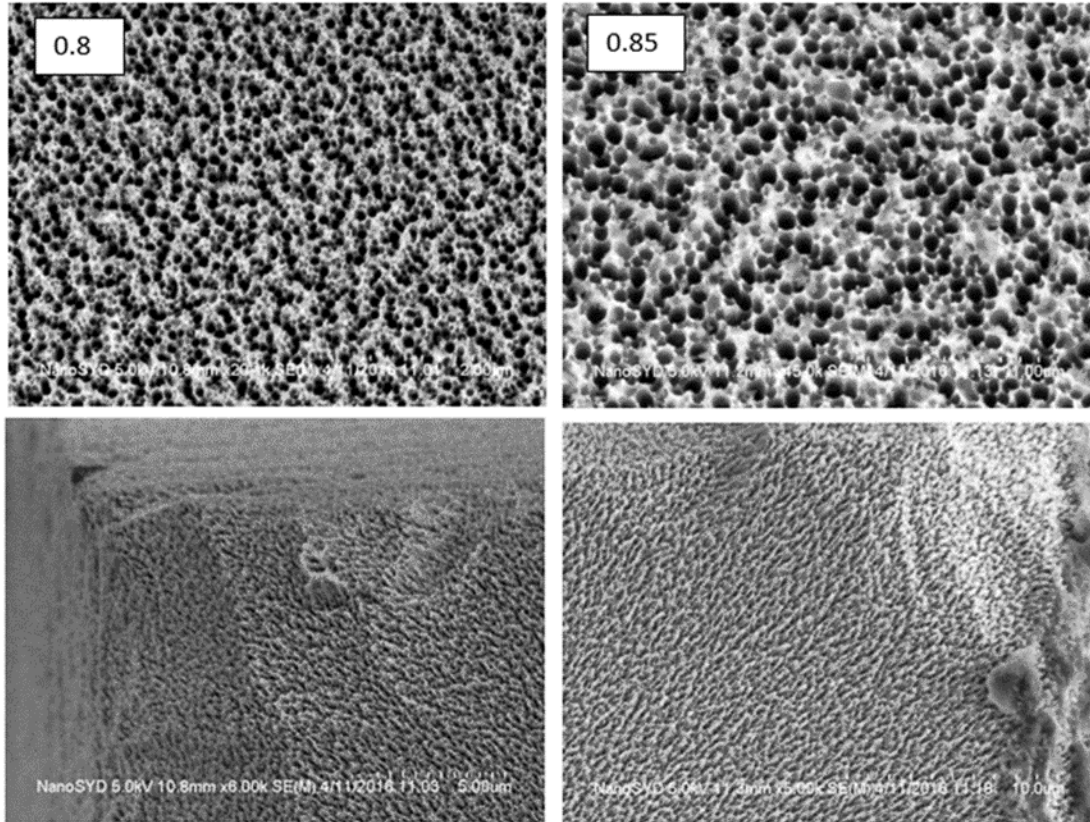
Figure 5.11 SEM top view images MCI NanoSYD

Respectively, for the side view the same procedure was done by cutting the samples after the top view done on SEM and after comparing the images, based on such features like: geometry of the grating, size, density etc. for the reflectivity measurements. In figure 5.11. are shown the SEM images from the side view of the samples with a lower ratio respectively α=0.75 and α=0.7 and the different in size between pillars is very small. And it is quite hard to understand which one has the lowest reflectivity rate.
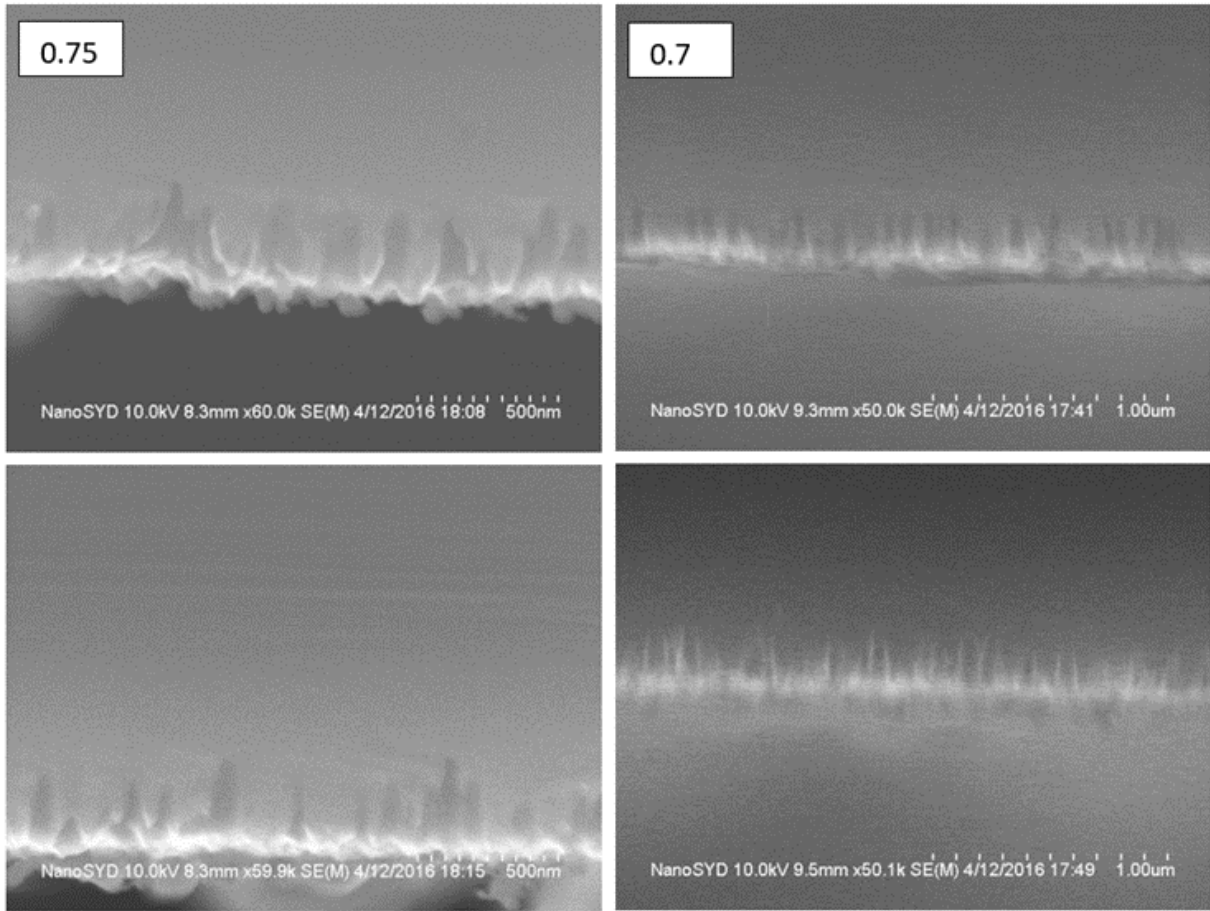
Figure 5.11 SEM side view images, MCI NanoSYD

In the figure 5.11 the pillars 'coming out' of the surface can be seen and same result is shown in the images from recipe α=0.8 - 0.85 are combined. Since the gas ratio between the recipes was small, this made the visual inspection hard to decide for the best sample. But going with the reflectivity rate it is more evident the light absorption scale in the samples.
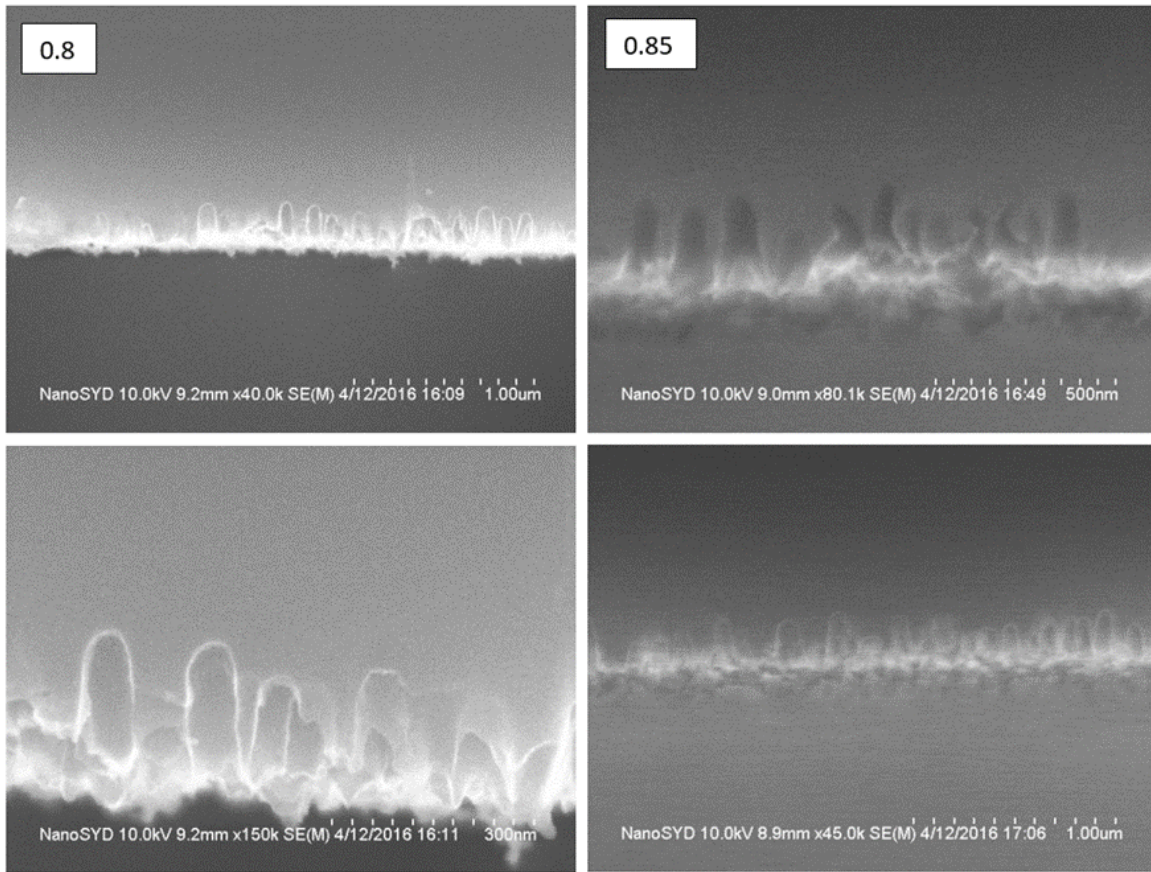
Table 5.3 SEM images side view MCI NanoSYD

It's possible to see that the top and side view images of these samples are clearer and the grating is more uniform across the area of the sample though between them; considering the images taken from the side view are evident some differences in terms of size and distribution of the trenches. Thought based on the images it is quite difficult to judge which sample(s) is the best and to avoid uncertainty to select the best sample, the reflectivity measurement took place. In the table below it is shown the respective reflection rate for each sample.

So, the ratio of gases combined in ICP RIE during etching process, results in different etching profiles due to the selectivity and dynamic of the process, influenced by the dominance or absence of one of the gases either SF_6 or O_2. Having more O_2 in the system will inhibit the etching process, thus increasing SF_6 level to stabilize the process and make it etch the silicon surface.

The opposite case is when there is a high amount of SF$_6$ gas, which will lead to a situation where the passivation layer will not be able to provide micro masks necessary to form the black silicon. For these reasons, finding the right equilibrium is theoretically easy to calculate but in practice is difficult to control and is difficult to understand the real process variables acting during the etching process. Concluding, on the studied case, the reflectivity levels were quite close as were closed also their ratio of gasses; all these considerations took the analysis to choose the part of the second stage gas ratios for the next samples; all is described in detail in the following chapters of this work.
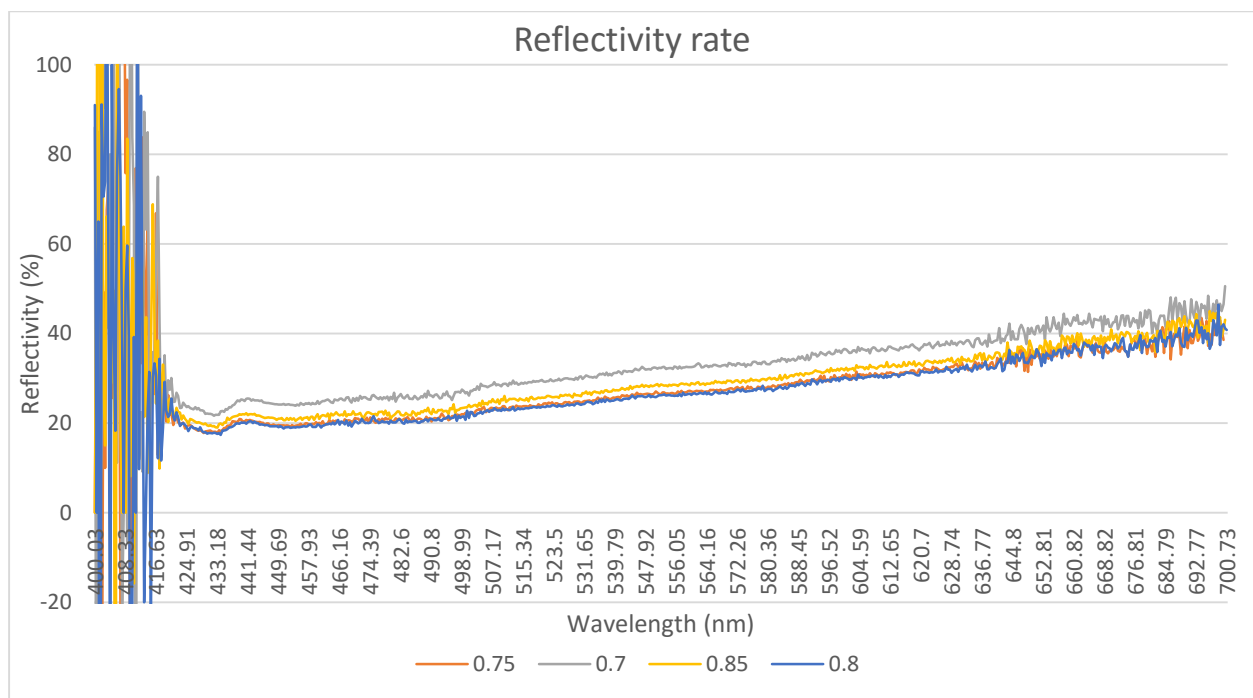

Figure 5.12 SEM Reflectivity MCI NanoSYD

5.5 Fourth stage

This step of the work was to find the best possible recipe to minimize the reflectivity level and, at this stage was introduced another variable to control: the chuck bias. The chuck bias, together with gas ratio, contributed with an additional change in the variables of the black silicon fabrication

Figure 5.13 Stage when Chuck bias power was introduced

Table 5.4 Table of variables changed

Ratio SF_6/O_2	SF_6 (sccm)	O_2 (sccm)	Chuck bias (W)	
	81.4	108.6	2	
0.75	81.4	108.6	4	**Derived from recipes 0.75-0.85**
	81.4	108.6	6	
	87.3	102.7	2	
0.85	87.3	102.7	4	
	87.3	102.7	6	

After all the recipes were executed, respectively with the ratios specified and including all the variables, was possible to acquire the following images from SEM.
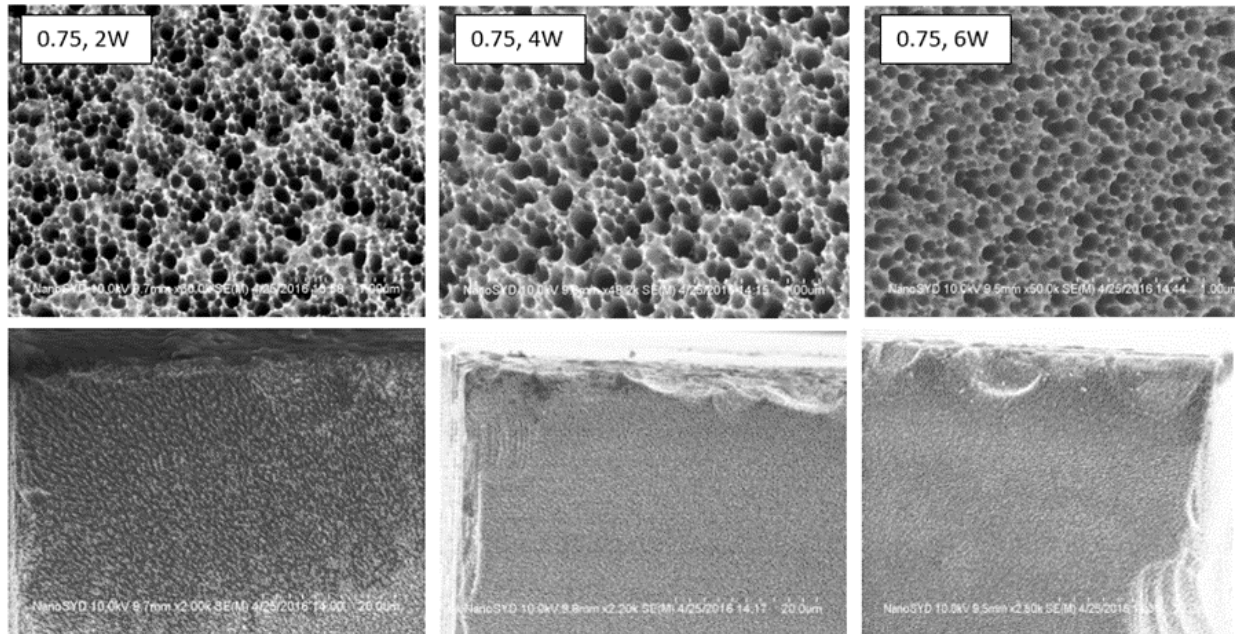

Figure 5.14 SEM top view images with different chuck bias power MCI NanoSYD

In figure 5.14 top view of SEM images is shown. For the other three samples with changed bias power level. Some impurities can be spotted in the samples; that are probably caused by the Ions hitting the surface and irregularities of the silicon crystal. Again here the pillar-like structures look regular in the scale of 1µm it is difficult to tell which sample will have the lowest reflectivity level or the best absorption rate.
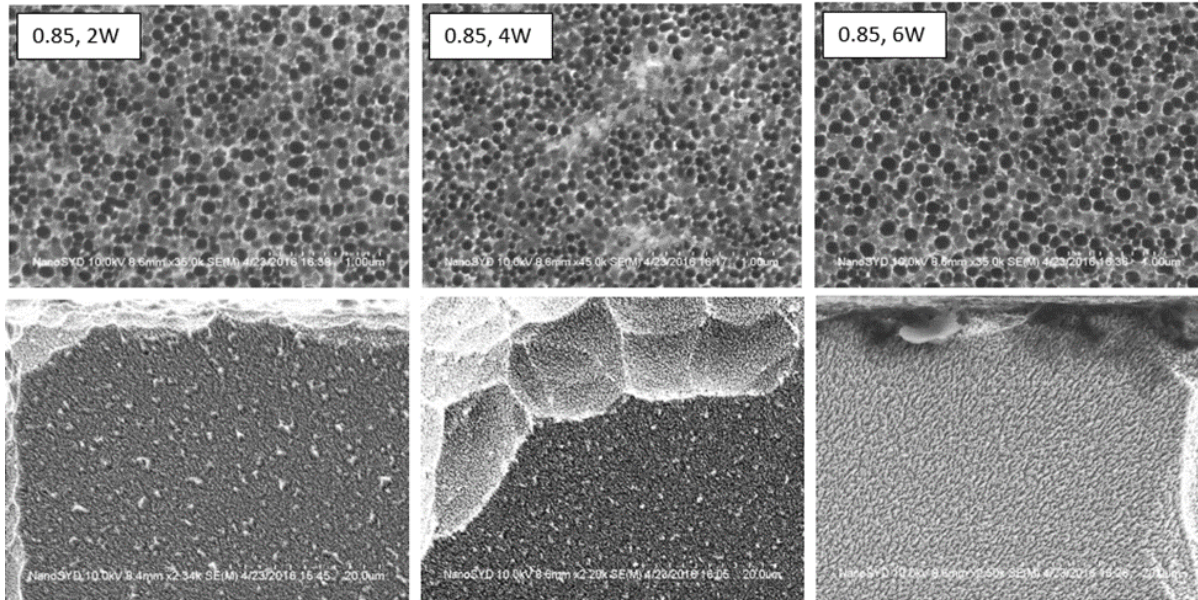
Figure 5.15 SEM Top View images

In figure 5.15 the top view of the samples with gas ratio α=0.85 treated at three different chuck bias power 2,46W. The results in microscale are also very similar for the second recipe set. It is visible that the cracks and not-finished structures in the corners of the samples which sometime create problems to take good side view images. Though for the top view they look similar still.

Below are shown the side view images of the sample respectively for each gas ratio combination, the images were taken under an undesired condition that is known as 'static build up charge' that basically makes the image to look blurry. Because it affects the backscattered electrons that are reflected back to the detector of SEM. By changing the energy level of the reflected electrons from the sample. Thus creating noise in the image but we can see that most of the samples where the side view is taken, have decent quality from SEM images.
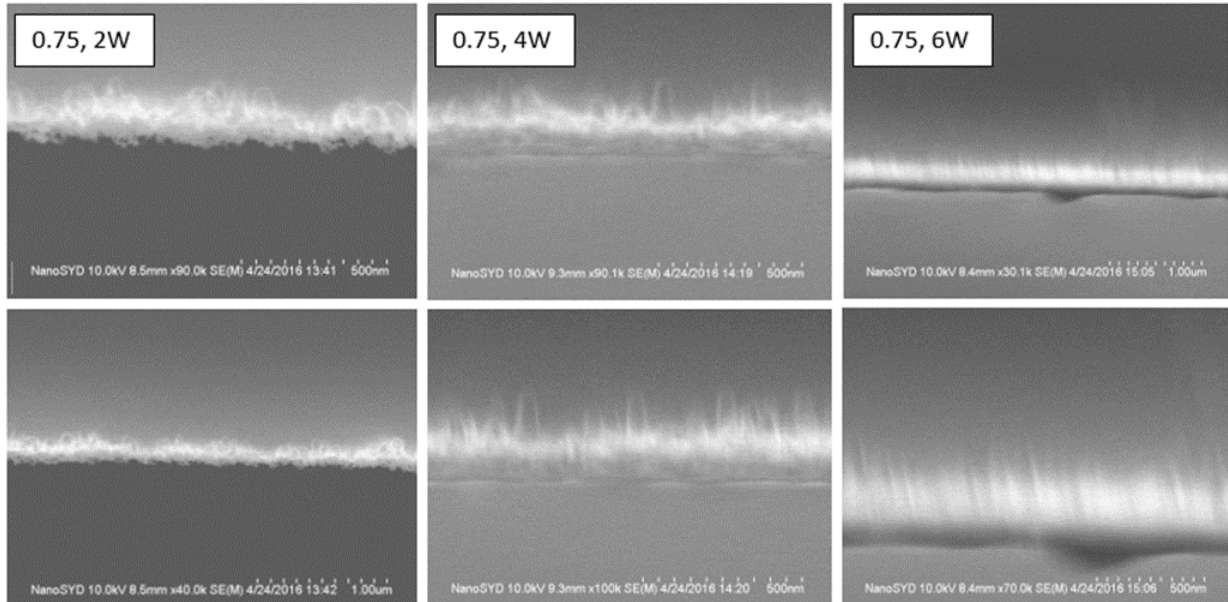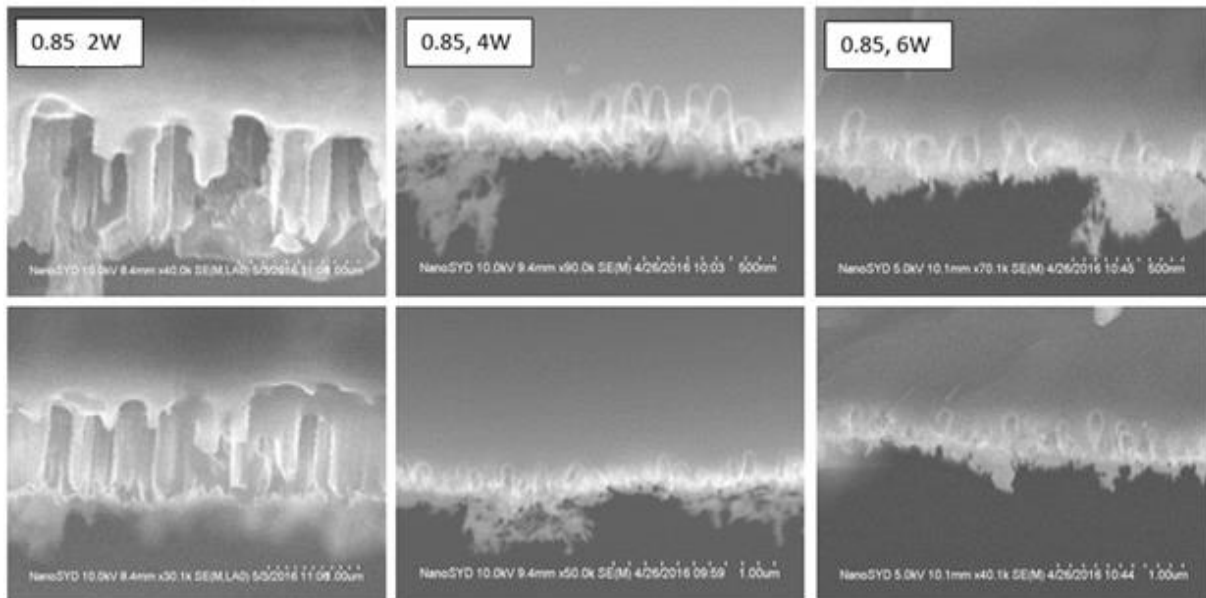
Figure 5.16 SEM side view images MCI NanoSYD

Figure 5.17 SEM side view images MCI NanoSYD

The reflectivity data from figure 5.18, acquired during this stage is the one where it is possible to understand the difference in the reflectivity level shown in the figure 5.18.
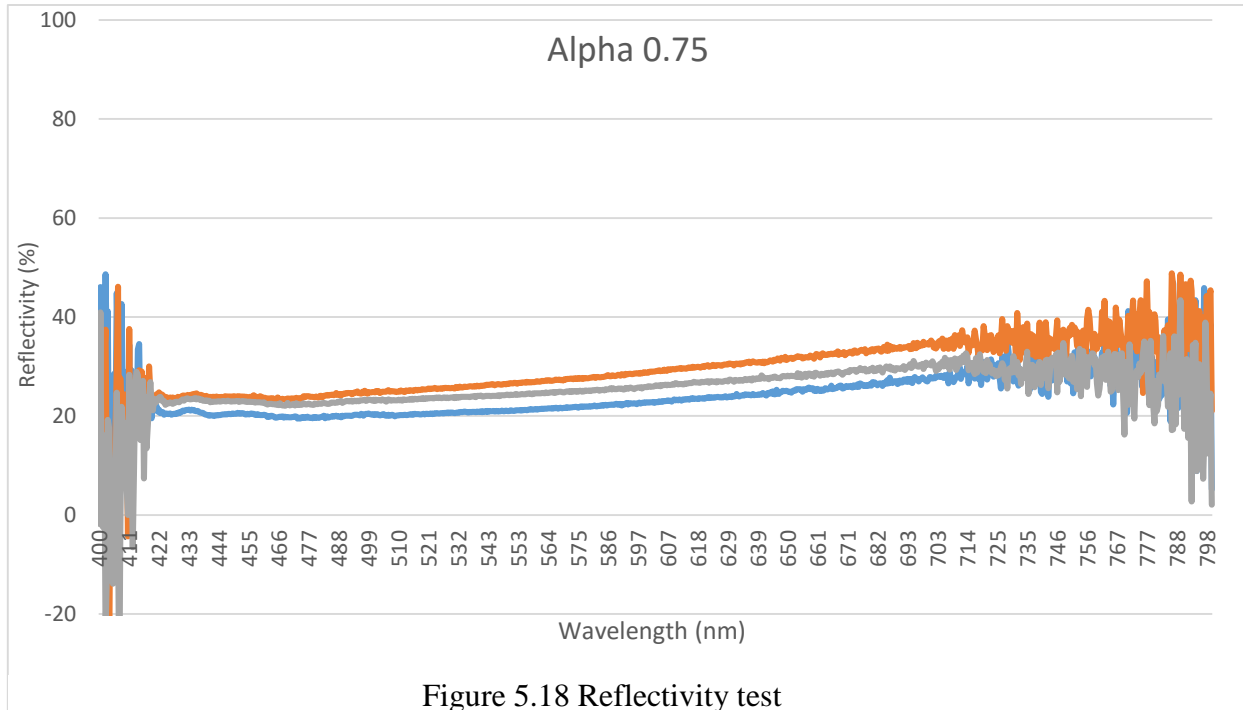

Figure 5.18 Reflectivity test

Going back to the SEM image analysis it was difficult to understand how the reflectivity rate differs from one sample to another. But from the data taken from the reflectivity test it is evident the difference in reflectivity rate from 400-700 nm is linear per each sample. And the one with the lowest reflectivity is sample with α=0.75 2W

To conclude, the behavior of all three samples is similar in the wavelength spectrum, from 400 to 700 nm. Considering the fact that the spectrometer range was from 165-1100 nm. So the reflectivity response is stable for a wide range of the wavelength, which is desirable though in a lower reflectivity level. Because in that way the aim of the work will be fulfilled with better results for the reflectivity level of the black silicon.
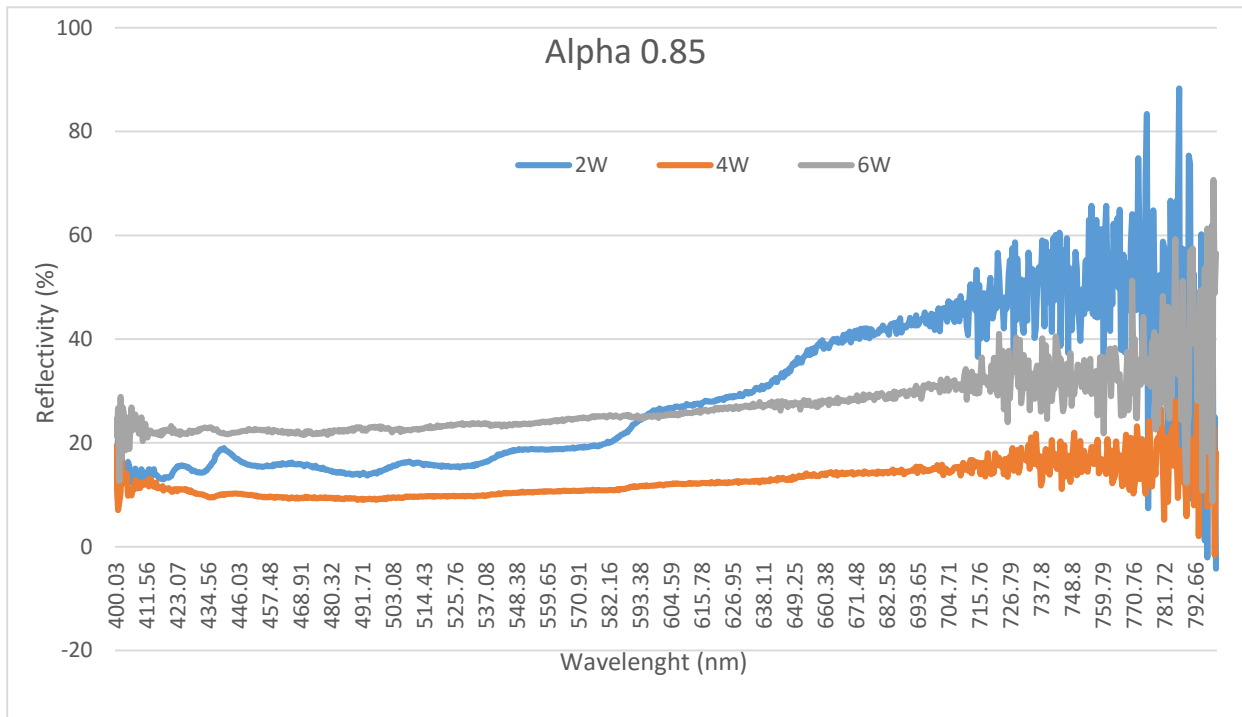
Figure 5.19 Reflectivity test

So, the best samples that have a low reflectivity level based on the graph are *0.75, 2W* with reflection value about *19% (from 400-500nm).* And for the second one as it is possible to refer to the figure 5.19, is the sample *0.85, 4W* with a reflectivity value around *10% (400-600nm)* the one chosen. It has an even lower reflectivity level in comparison from the chosen one on the first set. Though what is evident from both graphs, it is an improved light absorption from the samples after activating the chuck bias power. The reason why the reflectivity level changes and improves is because of the chuck bias power which, when applied at a low power level, can help remove some part of the passivation layer allowing the ions to etch deeper in the substrate; on the other hand, this is also by losing a bit the directionality of the etch process. Hence the structures that are deep and irregular in shape from SEM images. But what is important relies in the fact that the pillars will trap the incident light into the substrate while keeping the reflection levels low.

5.6 Fifth stage

After changing the chuck bias and picked three best samples selected on previous stages. At the last stage an additional process which is the Bosch process took place, with it the plan was to treat all the three best samples (two from the last recipe and one from the very first) and see the changes regarding the parameters interested, so for the start, with Bosch the final recipe with the following sample ratios shown on table 5.5:
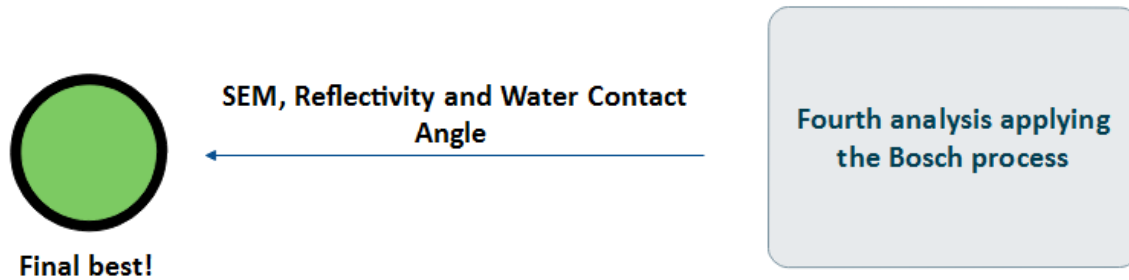
Figure 5.20 Final selection stage

Table 5.5 Table of gas ratios

Ratio SF_6/O_2	SF_6 (sccm)	O_2 (sccm)	Chuck power (W)
0.75	81.4	108.6	2
0.85	87.3	102.7	4
0.9	100	90	6

After applying these recipes in ICP RIE machine the new samples were directly sent them for the Bosch process to see its effect in microstructural level, according to the parameters shown from the table 5.5.

5.6.1 Bosch process

In this step after SEM and Reflectivity, best three samples out of nine were chosen. Top three samples were chosen after a series of selection previously, using Scanning Electron Microscopy images for the top and side view.
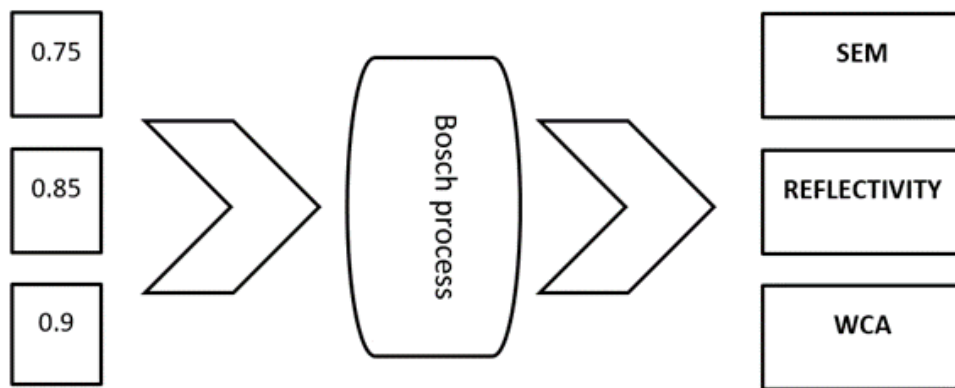

Figure 5.21 Applying Bosch on the selected samples

In the figure 5.21 is shown the schedule for the Bosch process, applied after the best sample was chosen, from recipe with $\alpha=0.75;0.85;0.9$. then the next steps were to test the results from the etching process in ICP RIE with SEM, Reflectivity test and introducing another testing step like Water Contact Angle (WCA) to measure the hydrophobicity of the surface.

So to this point it started first with acquiring the images from Scanning Electron Microscope respectively for the top and side view. Which this time surprisingly showed evident differences. From the top view, all the samples had an increase in size regarding the texture geometry and from the side view pillars looked like 'threaded' in the edges. For better understanding on the next page an overview of the images taken for top and side view is shown from SEM in figure 5.22.
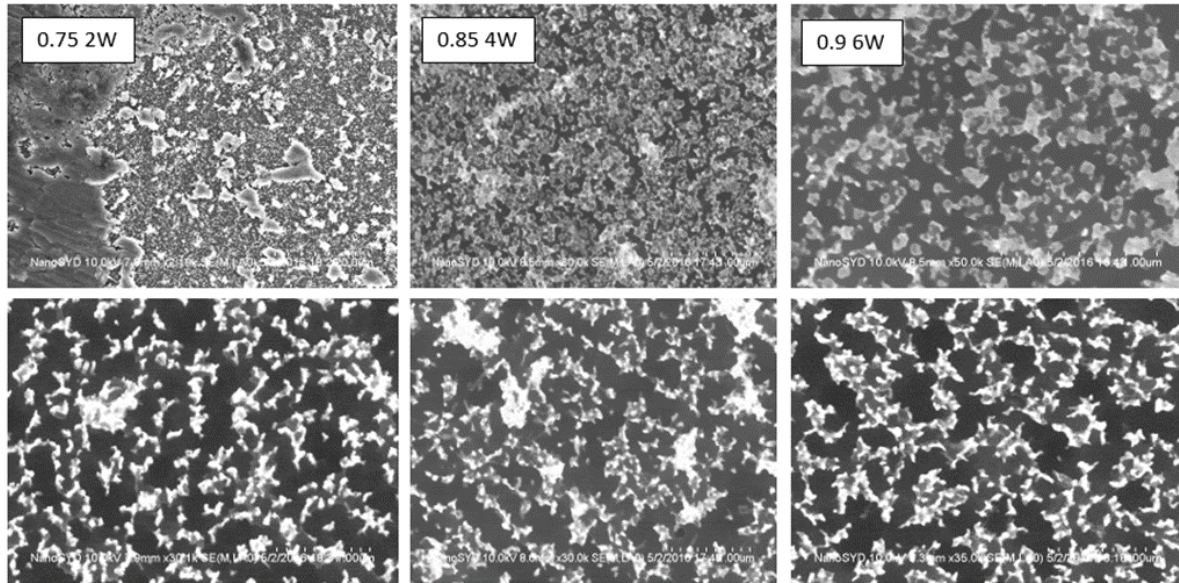
Figure 5.22 SEM top view images of the samples treated with Bosch process. MCI NanoSYD

For the side view, it's possible to see that the pillar's shape is improved and the height among them is similar which creates a good condition for hydrophobicity level, for which will be talking about later on. What is important to mention for the Bosch process, relies on the fact that all the structures that here look very irregular, when the side view was taken with SEM, the Nanostructures (pillars) were regular and uniformly spread around the sample.

The top view image shown the effect of the etching process which is able to act very strongly with the substrate, even for a short amount of time. Worth to mention here that the first test into applying Bosch to black silicon was run for 30 seconds. After the completion of the process the sample was completely wiped out from the nanostructures, it was as if someone cleaned the black silicon layer and made it with a clean surface again. So after that first test, we lowered the time for the Bosch process in 10 and 5 seconds, where the etching results were more effective.
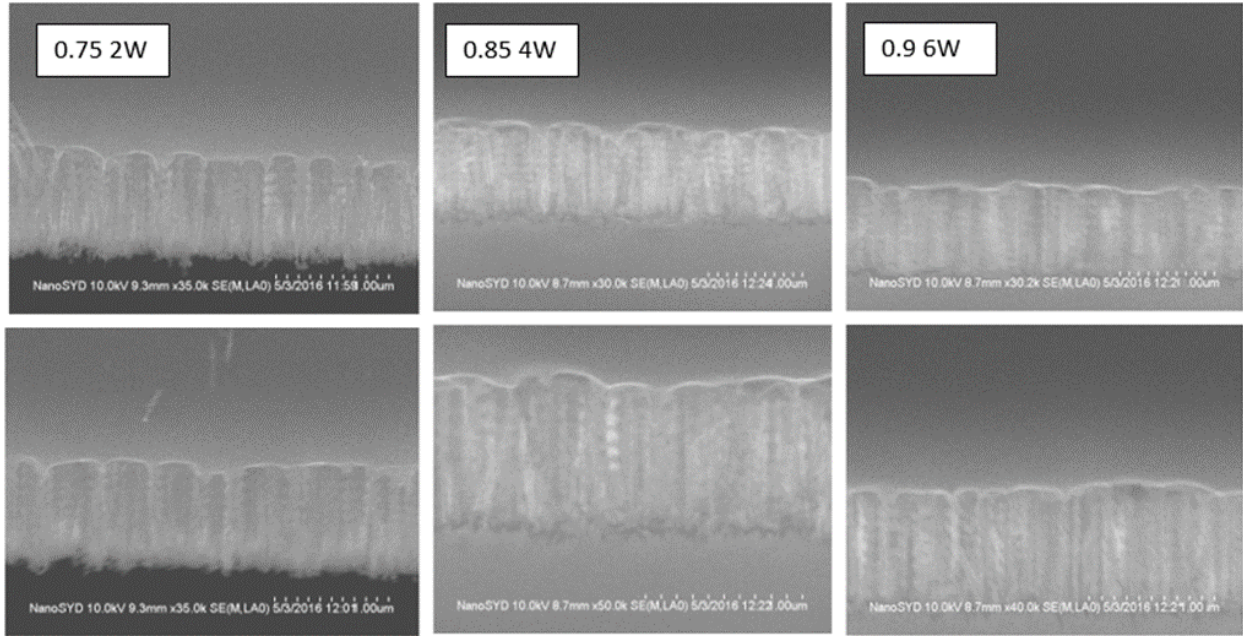
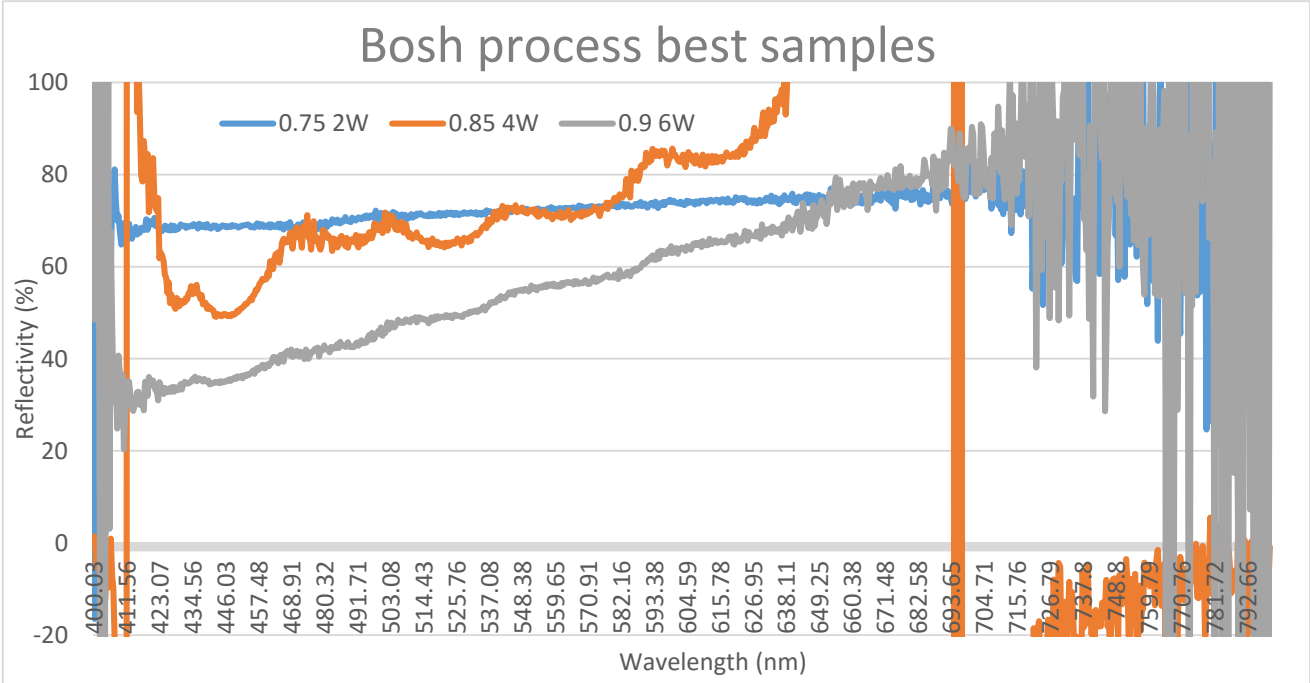Figure 5.23 SEM side view images treated with Bosch MCI NanoSYD

Figure 5.24 Reflectivity for the samples treated with Bosch

From figure 5.24 is shown the reflectivity level when applying Bosch changes dramatically to compare it with the previous samples, that have a reflectivity rate ranging from 10-20%. Here the absorption rate decreases quite two to three times the previous recipe. Thus the reflectivity rate for the Bosch process resulted too high so for the next test which was the WCA test. Where surprisingly other properties were exhibited on the samples treated with Bosch, this part will be discussed on the next part 5.6.2 with the Water Contact Measurement test.

5.6.2 Water contact angle

Finally, to test the effect of applying the Bosch process, the water contact angle test (WCA) was used to measure the other properties of samples treated with Bosch. surprisingly, when the set up was build that is quite similar to figure 5.25 a high contact angle for the treated samples was measured and almost not at all for the samples with only black silicon. So it was expected that WCA, would show us the hydrophobic properties of the black silicon as well, but the real test showed that black silicon not treated with Bosch did not have the property of being hydrophobic. Whereas the samples treated had it. Probably, the reason behind it is that the shape of the pillars is not completely evident in Bosch treated samples due to a large distance between the pillars.
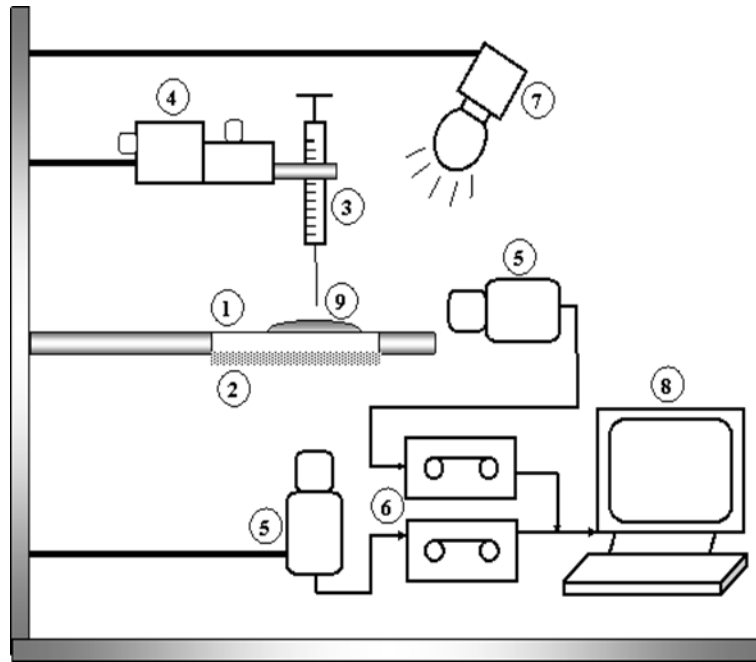
Figure 5.25 Water contact angle setup [34]

On the figure 5.26 the best black silicon sample treated at α=0.85 4W and from this test is difficult to distinguish the angle between the sample and the water surface it appears to be completely hydrophilic[6]. But when looking at the treated black silicon samples as in the figure 5.27 they will show a high level of hydrophobicity.

---

[6] The tendency to mix with/ dissolve in, or be wetted by water.
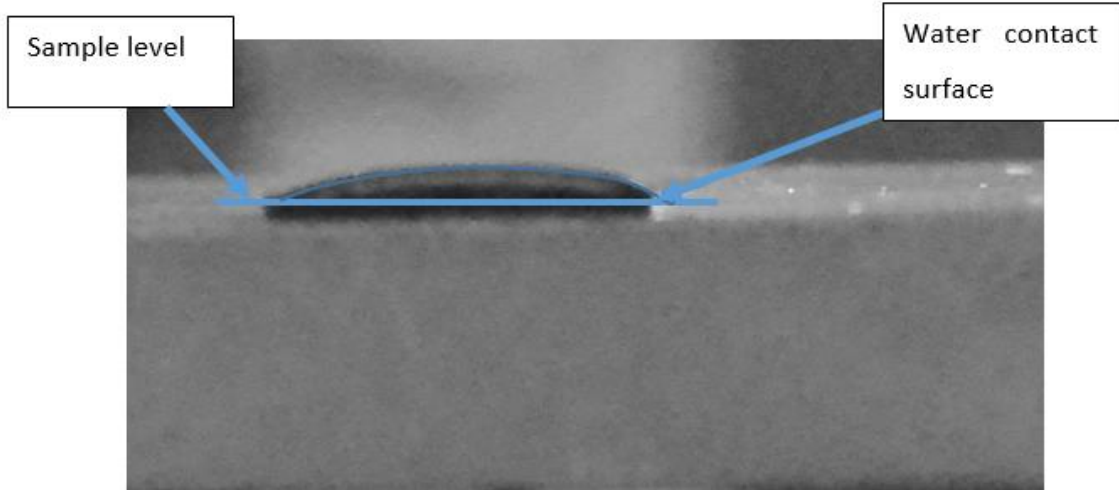
Figure 5.26 Hydrophobicity of the samples without Bosch process
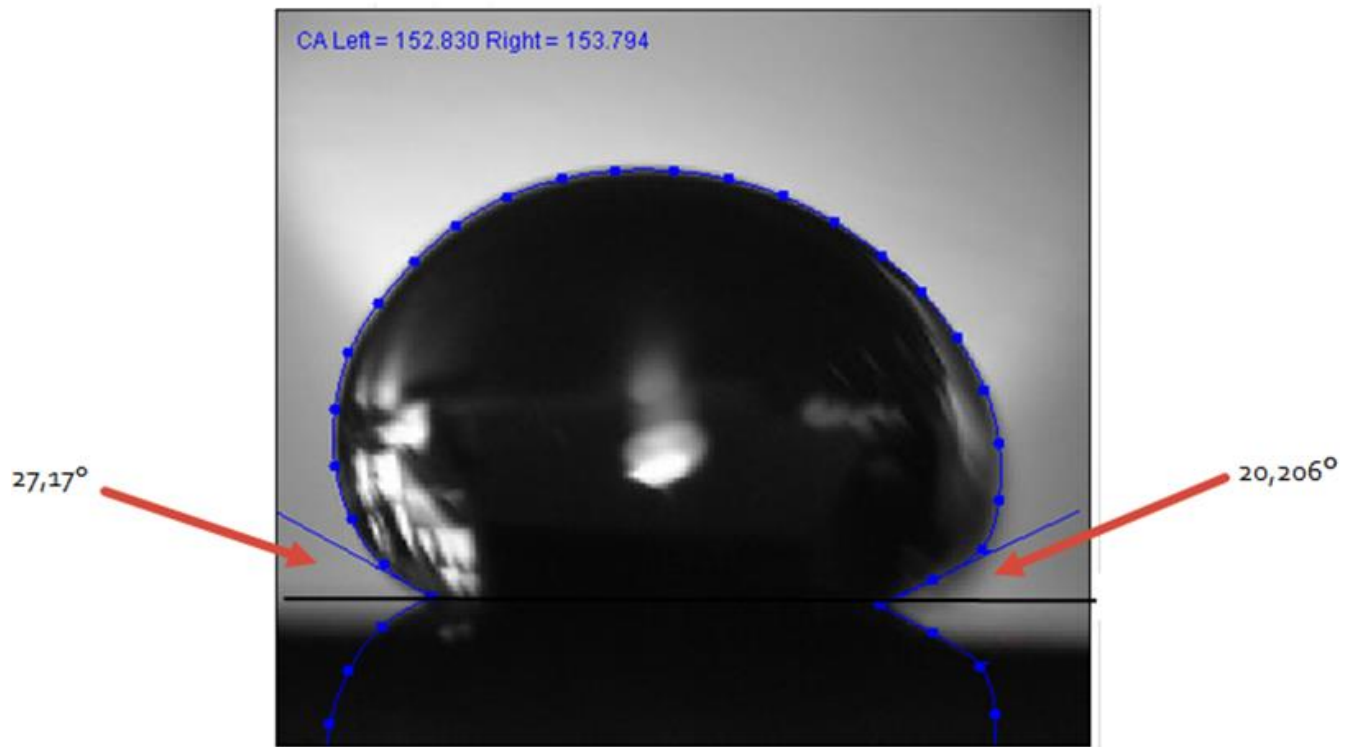
Figure 5.27 Hydrophobicity shown from samples treated with Bosch process

5.6.3 Hydrophobicity

Hydrophobicity is known to be a physical property of a molecule that can be repelled from a liquid mass or water, in case when no other repulsive forces are involved, in the figure 5.28 below are shown some basic measurements to calculate the contact angle which in our work is the main one used to measure the hydrophobicity of the surface for the Bosch treated black silicon samples.
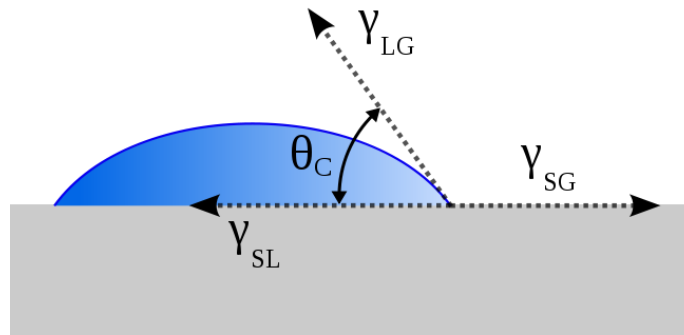
Figure 5.28 hydrophobicity contact angle [14]

Eq. 1
$$\gamma_{SG} = \gamma_{SL} + \gamma_{LG}\cos\theta$$

This is another image captured when testing hydrophobic properties of black silicon. By using the set-up mentioned at point 5.6.2

Figure 5.29 Hydrophobic properties of treated black silicon

5.7 Results and discussions

Through this work all the steps planned for an analysis of the black silicon fabrication procedures, analyzed the factors that affects its reflectivity rate. While trying and controlling different variables such as gas ratio, chuck bias power and finally apply the Bosch Process. The reason behind it was to understand what is the aim of this project into achieving a low-reflectivity level, and make the fabrication method available to the companies that produce solar cells. So that they can use the method of fabrication black silicon timewise with a lower cost which is one of the main advantages of black silicon in comparison with the gratings done in commercial solar cells.

All started with the best sample on the first stage with alpha 0.9 and went through a series of combination through the process to produce best samples from a close recipe, respectively $\alpha=0.75$ with chuck bias 4W and $\alpha=0.85$ with chuck bias 6W. and finally from these samples after acquiring the reflectivity test from $\alpha=0.85$ has the highest reflectivity rate. To apply the reflectivity test and measured once again reflectivity and introduced a new technique like hydrophobicity to measure the resistive hydrophobic properties of black silicon layer.

The work done through these steps exploited some solutions though limitations as well in the case of reflectivity drop when creating a hydrophobic surface. Worth to mention that the hydrophobicity effect is visible in the presence of short and thick pillar-like structures, just like in the lotus leaves [7]. The studied case, with the samples treated with Bosch process, is quite similar to the structures created by etching with Bosch. The sample treated in Figure 5.27 shows an angle of 155° approximately, and for this can be defined as super hydrophobic. The angle shown in the figure is complementary to the studied angle.

---

[7] A self-cleaning property that is a result of very high water repellence.

To conclude, the results from the study of black silicon production and application were close to the target result aiming at, either regarding SEM images, Reflectivity test and hydrophobicity. From all the data an indicator to a low reflectivity rate, the results from the reflectivity test were clearer, especially when applying Bosch process which as seen made the process to get worse. But what is important to conclude is the end results for the lowest reflectivity rate achieved, and that was from sample with α=0.85 4W. which according to the data gathered, it is the best one!

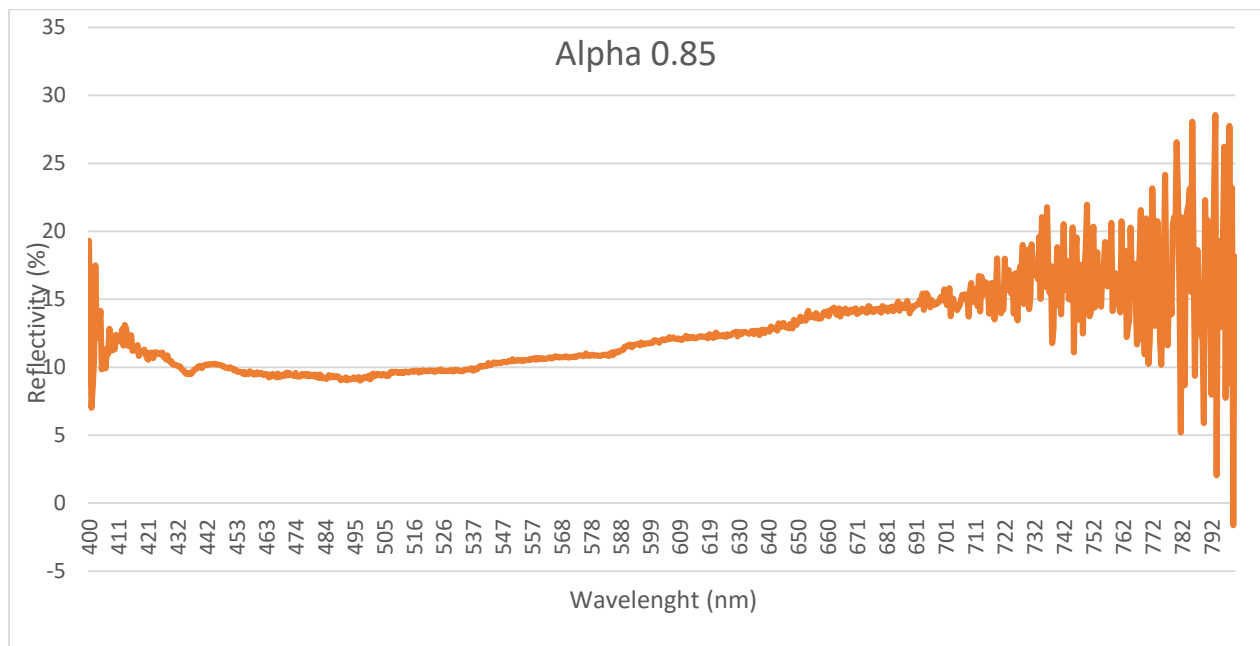Figure 5.30 Lowest reflectivity rate achieved, about 10% for the best sample with α=0.85, chuck bias 4W

6 Kokkuvõte JA EDASPIDINE TEGEVUS

Selles uurimuses valmistati musta silikooni meetodiga peegeldumisvastane kate. Tootmine toimus puhtaruumi keskonnas, ICP RIE plasma masinaga. Kasutatud meetod võimaldas meil luua ioonsöövitusprotsessiga(plasma etching process) nanostruktuurid, mis on vajalikud nende peale paigaldatud päiksepaneelidest peegeldumisvastase kihi jaoks. Selle töö teine lähenemine oli leida kõige efektiivsem meetod nanostruktuuride tootmiseks ja leida nende päikese neelamise võimekuse seotus nende suuruse, geomeetria ja tihedusega. Eesmärk on leida parim nanostruktuur, mis võimaldaks päikesepaneelidel võimalikult palju päikese energiat ammutada, kogudes hõlpsamini laenguid. Selle tulemusena koguneb rohkem elektrilist potentsiaali, kui päikesepaneelid on reastatud.

Musta silikooni moodustavate nanostruktuuride tootmiseks toodi sisse plasma etapp, meetod mis kasutab söövitamiseks ioone, mis on genereeritud plasma piirkonnas. Toore silikooni pinda pommitati ioonidega. Pommitamise sageduse kontrollimiseks (see on oluline naostruktuuride suuruse jaoks) mi toodis sisse kaks suurust. Üks suurustest on gaasi vahekord Sf_6 ja O_2 vahel ning teine chuck bias power, mis põhjustab söövitatava wafer'i peal rakendatava võimsuse. Nende kahe suuruse kombineerimisel plasma söövitus masinal loodi korralikud nanostruktuurid, millel on hea valguse neeldumis efektiivsus.

Lõppstaadiumis, pärast ioonsöövitusprotsessi rakendamist kontrollitud parameetritega, loodi näidised 10% peegeldumisega, mis tähendab 90 % valguse neeldumist. Enne selle tulemuseni jõudmist tekkis mitmeid probleeme. Mõned gaasi ja võimsuse kombinatsioonid viisid imelike nanostruktuuridega musta silikoonini. Selistel juhtudel peegeldumine ei vähenenud. Tähtsad parameetrid, mis võivad nanostruktuuride tekstuuri suurust, tihedust ja geomeetriat mõjutada, salvestati süsteemi. Need on musta silikooni kihi kvaliteedi juures olulised.

Protsessis esinesid mitmed piirangud: rakendatav gaasikogus, võimsus, söövitus aeg ja pommitamis sagedus. Iga muutuja kohta tehti eraldi test, muutes ainul tühte suurust ja hoides teisi fikseerituna. See oli ajakulukas protsess, et aru saada milline suurus on madala peegeldumisega struktuuri loomiseks oluline. Tulevikus on soovitatav kasutada arvutuslikke meetodeid, mis aitaks mõista valguse ja materjali vastastikust mõju. Seejärel luua suuruste jaoks kontrolliv algoritm, mis aitaks hea kvaliteediga peegeldumisvastast katet toota.

Selle töö tulemus aitas välja selgitada, mida peaks muutma, et saavutada päiksepaneelide väike peegelduvus. Paremat valguse neeldumist saab saavutada, kui geomeetrilised tegurid ja valguse omadused on teada. See julgustab meid viima musta silikooni meetodit järgmisele staadiumile. Söövitusparameetreite, nanostruktuuride geomeetria ja teiste kontroll suuruste kontrollimine võib viia parema efektiivsuse ja madalama hinnaga päikesepaneelideni, mis oleksid majanduslikult hea hinnaga ning sobiksid eri liiki klientidele.

7   SUMMARY AND FUTURE WORK

In this work, the study consisted on the fabrication of an antireflection layer using the black silicon method, done in the cleanroom environment using ICP RIE plasma machine. The method used, allowed us to create the Nanostructures from plasma etching process, necessary for the anti-reflective layer of solar cells that is placed on top of it. Another approach to this work was to find the most efficient way to fabricate the Nanostructures, and to find the relationship between their size, geometry and density with the ability to absorb the light. The reason behind it is to find the best Nano-shape(s) that could potentially harvest the photonic energy, that is hitting the surface of the solar cells allowing the charges (electron-hole pair) to build up more easily. This leads to producing a higher electrical potential when the solar cells are combined together in an array.

To fabricate the Nanostructures, forming the black silicon, the plasma stage was introduced, as a method that uses ions for etching, generated at plasma region. With it, the surface of a raw silicon was bombarded with ions. For controlling the bombardment rate, important for the size and shape of these Nano-structures, two variables were introduced. One of them was the gas ratio between Sf6 and O2 and the other, chuck bias power (W), responsible for the potential applied on the wafer that is being etched. By combining these variables in the plasma etching machine, decent Nanostructures were created with good efficiency for the light absorption.

In the end stage after applying the plasma etching process with controlled parameters, samples with reflectivity rate of 10% were created, this translates to about 90% light absorption. Though into reaching this result different issues and failures were faced, i.e. some gas and power combination resulted into a poor black silicon or strange micro-shapes that were not contributing into lowering the reflectivity. Albeit, in the end, important parameters that could potentially affect the size, density and geometry of the textures, important for a quality black silicon layer, were logged in the system.

Some limitations during this process were also present, and in different directions, starting from the amount of gas that could be applied, the power, etching time and the bombardment rate. For each variable, the test was done separately, by changing only one variable while keeping others fixed. This procedure was potentially time-consuming, into understanding which variable is more important to achieve such geometry so that the reflectivity rate is very low. So, for a possible perspective work and better results, going with a computational method that could understand the aspects of light-matter interaction, and then create a control algorithm for the variables would be a possible solution into fabricating a good quality anti-reflection layer.

To conclude, the results from this work were promising into understanding what should be changed to achieve a good anti-reflection layer in the solar cells. Also, it proved that when the geometrical factors and light properties are understandable to us, better results can be achieved in the light absorption rate. This encourages us to move the black silicon method forward to the next progress point. Where, applying it timewise, controlling etching variables, Nanostructures geometry and control parameters, could lead to potentially better efficient and low-cost solar cell products that can be commercially affordable for different categories of customers.

8 REFERENCES

[1]   V. R. Manfrinato, L. Zhang, D. Su, H. Duan, R. G. Hobbs, E. A. Stach, and K. K. Berggren, "Resolution Limits of Electron-Beam Lithography toward the Atomic Scale," *Nano Lett.*, vol. 13, no. 4, pp. 1555–1558, 2013.

[2]   J. Melorose, R. Perroy, and S. Careas, "No Title No Title," *Statew. Agric. L. Use Baseline 2015*, vol. 1, 2015.

[3]   A. N. Broers, A. C. F. Hoole Andrew C.F, and J. M. Ryan, "Electron beam lithography - Resolution limits," *Microelectron. Eng.*, vol. 32, no. 1–4 SPEC. ISS., pp. 131–142, 1996.

[4]   S. Y. Chou, "Sub-10 nm imprint lithography and applications," *J. Vac. Sci. Technol. B Microelectron. Nanom. Struct.*, vol. 15, no. 6, p. 2897, Nov. 1997.

[5]   A. Vaseashta and D. Dimova-Malinovska, "Nanostructured and nanoscale devices, sensors and detectors," *Sci. Technol. Adv. Mater.*, vol. 6, no. 3–4, pp. 312–318, Apr. 2005.

[6]   S. J. Randolph, J. D. Fowlkes, and P. D. Rack, "Focused, Nanoscale Electron-Beam-Induced Deposition and Etching," *Crit. Rev. Solid State Mater. Sci.*, vol. 31, no. 3, pp. 55–89, 2006.

[7]   Ü. Sökmen, A. Stranz, S. Fündling, H.-H. Wehmann, V. Bandalo, A. Bora, M. Tornow, A. Waag, and E. Peiner, "Capabilities of ICP-RIE cryogenic dry etching of silicon: review of exemplary microstructures," *J. Micromechanics Microengineering*, vol. 19, no. 10, p. 105005, 2009.

[8]   R. . Shul, G. . Vawter, C. . Willison, M. . Bridges, J. . Lee, S. . Pearton, and C. . Abernathy, "Comparison of plasma etch techniques for III–V nitrides," *Solid. State. Electron.*, vol. 42, no. 12, pp. 2259–2267, Dec. 1998.

[9]   C. Chang, Y.-F. Wang, Y. Kanamori, J.-J. Shih, Y. Kawai, C.-K. Lee, K.-C. Wu, and M. Esashi, "Etching submicrometer trenches by using the Bosch process and its application to the fabrication of antireflection structures," *J. Micromechanics Microengineering*, vol. 15, no. 3, p. 580, 2005.

[10]   M. Horodecki and J. Oppenheim, "Fundamental limitations for quantum and nanoscale thermodynamics.," *Nat. Commun.*, vol. 4, no. May, p. 2059, 2013.

[11]   J. J. Sakurai and J. Napolitano, *Modern quantum mechanics; 2nd ed.* San Francisco, CA: Addison-Wesley, 2011.

[12]   G. Binnig and H. Rohrer, "Scanning tunneling microscopy," *Surf. Sci.*, vol. 126, no. 126, pp. 236–244, 1982.

[13]   H. Zhou, Q. Chen, G. Li, S. Luo, T. Song, H.-S. Duan, Z. Hong, J. You, Y. Liu, and Y. Yang, "Interface engineering of highly efficient perovskite solar cells," *Science (80-.).*, vol. 345, no. 6196, pp. 542–546, 2014.

[14]   S. A. Campbell, *Fabrication Engineering at the Micro- and Nanoscale*. Oxford University Press, 2013.

[15] R. Brendel, R. Auer, and H. Artmann, "Textured monocrystalline thin-film Si cells from the porous silicon (PSI) process," *Prog. Photovoltaics Res. Appl.*, vol. 9, no. 3, pp. 217–221, 2001.

[16] "RPI SCOREC - Plasma Etch Modeling." [Online]. Available: http://www.scorec.rpi.edu/research_plasmaetchmodeling.php. [Accessed: 2-May-2016].

[17] M. Moreno, D. Daineka, and P. Roca i Cabarrocas, "Plasma texturing for silicon solar cells: From pyramids to inverted pyramids-like structures," *Sol. Energy Mater. Sol. Cells*, vol. 94, no. 5, pp. 733–737, May 2010.

[18] a. Deraoui, A. Balhamri, M. Rattal, Y. Bahou, A. Tabyaoui, M. Harmouchi, A. Mouhsen, and E. M. Oualim, "Black Silicon: Microfabrication Techniques and Characterization for Solar Cells Applications," *Int. J. Energy Sci.*, vol. 3, no. 6, pp. 403–407, 2013.

[19] N. Cheung and U. C. Berkeley, "Solar Cells Fabrication Technologies Crystalline Si Cell Technologies Amorphous Si Cell Technologies Thin Film Cell Technologies For a comprehensive tutorial on solar cells in general, Source : World Energy Council."

[20] E. Vazsonyi, K. De Clercq, R. Einhaus, E. Van Kerschaver, K. Said, J. Poortmans, J. Szlufcik, and J. Nijs, "Improved anisotropic etching process for industrial texturing of silicon solar cells," *Sol. Energy Mater. Sol. Cells*, vol. 57, no. 2, pp. 179–188, Feb. 1999.

[21] M. Kroll, M. Otto, T. Käsebier, K. Füchsel, R. B. Wehrspohn, E.-B. Kley, A. Tünnermann, and T. Pertsch, "Black silicon for solar cell applications," *Proc. SPIE*, vol. 8438, no. 8438–42, p. 843817, 2012.

[22] P. Panek, M. Lipiński, and J. Dutkiewicz, "Texturization of multicrystalline silicon by wet chemical etching for silicon solar cells," *J. Mater. Sci.*, vol. 40, no. 6, pp. 1459–1463, 2005.

[23] X. Li, T. Abe, and M. Esashi, "Deep reactive ion etching of Pyrex glass using SF6 plasma," *Sensors Actuators A Phys.*, vol. 87, no. 3, pp. 139–145, Jan. 2001.

[24] X. Liu, P. R. Coxon, M. Peters, B. Hoex, J. M. Cole, and D. J. Fray, "Black silicon: fabrication methods, properties and solar energy applications," *Energy Environ. Sci.*, vol. 7, no. 10, pp. 3223–3263, 2014.

[25] "Plasma Etcher." [Online]. Available: https://www.crystec.com/trietche.htm. [Accessed: 01-Apr-2016].

[26] "Dry Etching (ICP RIE) - NanoSYD Cleanroom." [Online]. Available: http://nanosyd.dk/cleanroom/en/page/dry-etching-icp-rie. [Accessed: 27-May-2016].

[27] H. Jansen, M. de Boer, J. Burger, R. Legtenberg, and M. Elwenspoek, "The black silicon method II:The effect of mask material and loading on the reactive ion etching of deep silicon trenches," *Microelectron. Eng.*, vol. 27, no. 1–4, pp. 475–480, 1995.

[28] "ICP basics." [Online]. Available: http://ireap.umd.edu/ppm/Papers/JVA00239.pdf. [Accessed: 15-May-2016].

[29] T. Saga, "Advances in crystalline silicon solar cell technology for industrial mass production," *NPG Asia Mater.*, vol. 2, no. 3, pp. 96–102, 2010.

[30] "Black Silicon Solar - Home." [Online]. Available: http://www.blacksiliconsolar.com/. [Accessed: 31-Mar-2016].

[31] Nanotechnology Fabrication Lab "::NANOFAB CENTER::" [Online]. Available: https://www.nnfc.re.kr/eng/U_service/03_equipment_v.jsp?seq=95&gubn [Accessed: 7-May-2016].

[32] "Scanning electron microscope - NanoSYD Cleanroom." [Online]. Available: http://nanosyd.dk/cleanroom/en/page/sem. [Accessed: 9-May-2016].

[33] SEM Handbook "Scanning Electron Microscopy Primer." [Online]. Available: http://www.charfac.umn.edu/sem_primer.pdf. [Accessed: 10-May-2016].

[34] "Determination of Contact Angle from Contact Area of Liquid Droplet Spreading on Solid Substrate from Leonardo Electronic Journal of Practices and Technologies." [Online]. Available: http://lejpt.academicdirect.org/A10/029_038.htm. [Accessed: 10-May-2016].

9 APPENDENCES

Table 9.1 Energy spent for solar cell production

Material	Energy content	Energy payback time
EG Silicon	200kWh/kg	Monocrystalline Si cell
Solar Grade Si	50Wh/kg	Polycrystalline Si cell
MG silicon	20Wh/kg	Amorphous Si cell

Table 9.2 coating methods in solar cell fabrication

Criteria	Coating	Surface passivation	Metallization mask	Chemical resistance	High-temperature stability	Cost and throughput	Overall rating
SiO2	Poor	Excellent	Very good	Very good	Very good	Poor?	Good
Si3N4	Very good	Very good	Excellent	Excellent	Very good	Average	Excellent
CeO2	Excellent	Average	Good	Unknown	Unknown	Good?	Very good
SiON	Average	Poor	Very good	Very good	Very good	Poor	average

Table 9.3 Size of the pillars after plasma treatment

	Height nm (from 1-5)	Width nm from (6-10)
Sample α=0.75	3.125	1.007
	3.236	1.124
	3.424	1.299
	3.444	0.943
	3.061	0.708

Table 9.4 Water contact angle for three different recipes

Alpha α	Left contact angle	right contact angle
α=0.75	152.8	153.7
α=0.85	149	150.1
α=0.9	148.5	149.2